JPRS L/9721

8 May 1981

USSR Report

EARTH SCIENCES

(FOUO 4/81)

FBIS FOREIGN BROADCAST INFORMATION SERVICE

FOR OFFICIAL USE ONLY

APPROVED FOR RELEASE: 2007/02/08: CIA-RDP82-00850R000400010017-8

NOTE

JPRS publications contain information primarily from foreign newspapers, periodicals and books, but also from news agency transmissions and broadcasts. Materials from foreign-language sources are translated; those from English-language sources are transcribed or reprinted, with the original phrasing and other characteristics retained.

Headlines, editorial reports, and material enclosed in brackets [] are supplied by JPRS. Processing indicators such as [Text] or [Excerpt] in the first line of each item, or following the last line of a brief, indicate how the original information was processed. Where no processing indicator is given, the information was summarized or extracted.

Unfamiliar names rendered phonetically or transliterated are enclosed in parentheses. Words or names preceded by a question mark and enclosed in parentheses were not clear in the original but have been supplied as appropriate in context. Other unattributed parenthetical notes within the body of an item originate with the source. Times within items are as given by source.

The contents of this publication in no way represent the policies, views or attitudes of the U.S. Government.

APPROVED FOR RELEASE: 2007/02/08: CIA-RDP82-00850R000400010017-8

JPRS L/9721

8 May 1981

USSR REPORT
EARTH SCIENCES
(FOUO 4/81)

CONTENTS

OCEANOGRAPHY

UDC 551.466.8(261)

MODEL OF THE FREQUENCY SPECTRUM OF INTERNAL WAVES IN THE OCEAN

Moscow IZVESTIYA AKADEMII NAUK SSSR: FIZIKA ATMOSFERY I OKEANA in Russian Vol 17, No 1, Jan 81 pp 67-75

[Article by K. D. Sabinin and V. A. Shulepov, Acoustics Institute USSR Academy of Sciences, manuscript submitted 2 Oct 79]

[Text]

Abstract: A comparison of the experimental frequency spectra measured on expeditions of the Acoustics Institute using the Garrett-Munk model indicates the existence of two special parts of the spectrum in which peaks of tidal and short-period internal waves rise over the monotonically decreasing background part. There is a difference in the spectral levels of the model and the background of the experimental spectra in the equatorial latitudes. A somewhat modified model of the background part of the frequency spectrum is proposed in which the nondependence of the spectral level on geographical latitude is assumed. Some characteristics of short-period internal waves are discussed.

According to the Garrett-Munk model, the frequency spectrum of the vertical displacements ζ in internal waves has the form:

$$S_\zeta(f, z)=CN^{-1}(z)f_i f^{-3}\sqrt{f^2-f_i^2}\ \text{м}^2\cdot\text{ч}, \qquad (1)$$

where C = 204 $m^2 \cdot hr^{-1}$; N(z) is the local Väisälä frequency; f_1 is the inertial frequency [1, 2].

A comparison of the frequency spectra of temperature fluctuations in the upper thermocline which we measured in a number of regions of the world ocean with model (1) indicated that the rate of dropoff of the spectrum with frequency in the region of the spectral continuum (background) predicted by the model agrees well with the results of the measurements in [3]. Major discrepancies are observed in two frequency regions -- at tidal and high (near the local Väisälä frequency) frequencies, where the experimental spectra have peaks. With respect to the absolute spectral levels of the background, the data from point temperature detectors (photothermographs, etc.), which constitute the greater part of the data which we

analyzed, do not make possible evaluation of the vertical displacements of the thermocline with an accuracy necessary for studying the geographical variability of the spectral levels [3].

Distributed temperature sensors give more reliable information for the corresponding evaluations [4]. The measurements made using these sensors in the Sargasso Sea and two equatorial regions of the Indian Ocean -- the Seychelles and the Maldives [3, 5] -- revealed a beautiful coincidence with the Garrett-Munk model in the Sargasso Sea and large discrepancies in the low latitudes, where the experimental spectral levels were much higher than those predicted by the model. This result is illustrated in Fig. 1, which shows the spectra of vertical displacements of the thermocline in the Seychelles and Maldives polygons. The measurements were made using four 100-m temperature sensors, which were situated at the center of the upper thermocline (40-100 m in the Seychelles region and 50-150 m in the Maldives region) [5]. The solid curves represent the spectra corresponding to the first 17-hour segments of the measurements; the dashed curves represent the second segments of the same duration. The spectra computed using formula (1) are shown in the form of solid sloping straight lines. It can be seen that the law of decrease of all the spectra is identical, but the Garrett-Munk spectrum is 12 db lower than the level of the experimental spectra. The spectrum of the first segment of the Seychelles measurements has a peak at a frequency of 3 cycles$\cdot$hr^{-1}, rising above the background, for which the one can use the spectrum of the second segment, by 9 db.

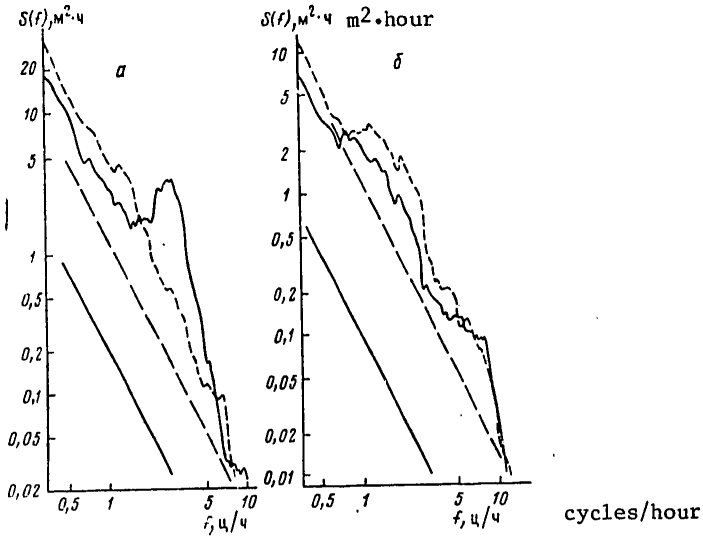

Fig. 1. Spectra of vertical displacements of thermocline in the Seychelles (a) and Maldives (b) regions.

It can be postulated that the extrapolation of the conclusions drawn by Garrett and Munk on the basis of measurements in the extratropical latitudes is not entirely correct for the low latitudes since it gives considerably understated spectral

levels. The approximation of the experimental spectra of vertical displacements is improved if model (1) is somewhat modified, assuming that the spectral levels at frequencies considerably greater than the local inertial frequency are not dependent on geographical latitude:

$$S_\zeta(f, z)=C_1N^{-1}(z)f^{-3}\sqrt{f^2-f_i^2}. \quad (2)$$

Here C_1 is some constant whose value can be found, taking into account the good correspondence of the experimental data and model (1) in the subtropical latitudes: $C_1 = Cf_i = 204\ m^2\cdot hour^{-1}\cdot 0.042\ cycle\cdot hour^{-1} = 8.5\ m^2\cdot hour^2$ (0.042 cycle·hour^{-1} is the inertial frequency at 30° latitude). The corresponding spectra, illustrated in Fig. 1 by sloping dashed lines, far better agree with the experimental data for the Seychelles and Maldives regions.

Since the range of free internal waves (from f_i to N) broadens with a decrease in geographical latitude and a nondependence of the high-frequency part of the spectrum on the inertial frequency means that the total energy of the internal waves does not remain constant and is equal to 0.4 J·cm^{-2}, as was postulated by Garrett and Munk, but changes with latitude. In actuality, according to [2], the dimensionless energy $\hat{E}$ of internal waves in a column of water of a unit section is

$$\hat{E}=\int_0^\infty\int\hat{E}(\alpha,\omega)\,d\alpha\,d\omega=\int_0^\infty\int\hat{E}A(\lambda)B(\omega)\,d\lambda\,d\omega, \quad (3)$$

where $B(\omega) = 2\pi^{-1}\omega_i\omega^{-1}(\omega^2-\omega_i^2)^{-1/2}$; ω and ω_i are the dimensionless current and local inertial frequencies; α and λ are dimensionless wave numbers; λ is normalized in such a way that

$$\int_0^\infty A(\lambda)\,d\lambda = 1.$$

Similarly

$$\int_0^\infty B(\omega)\,d\omega = 1.$$

The replacement of the product Cf_i into expression (1) by the constant value Cf_i (30°) = 8.5 m^2·hour^{-2} is equivalent to the introduction of the new frequency function $B'(\omega) = C_2B(\omega)\omega_i^{-1}$, as a result of which in place of

$$\int_0^\infty B(\omega)\,d\omega = 1 \text{ we have } \int_0^\infty B'(\omega)\,d\omega = C_2/\omega_i,$$

that is, the expression for energy (3) becomes dependent on the inertial frequency: $\hat{E}' = C_2\hat{E}\omega_i^{-1}$.

Since at latitude 30° the Garrett-Munk model describes the spectrum of internal waves well, it can be assumed that $C_2 = \omega_i(30°)$, from which, converting to dimensional values, we obtain the following expression for the dependence of the energy of internal waves on geographical latitude φ (for $\varphi > 0$):

$$E=0{,}2/\sin\varphi \ \ J\cdot cm^{-2}. \quad (4)$$

[Note: Using the estimate of the kinetic energy of the quasistationary circulation of the world ocean from [6] (10^{18} J) and relating it to a column of water with a section 1 cm^2 -- 10^{18} J/3.61·10^{18} $cm^2 \approx 0.3$ J·cm^{-2}, we find that in the low latitudes this is much less than the total energy of the internal waves (with $\varphi = 5°$, for example, E = 2.2 J·cm^{-2}), although it must be remembered that the intensity of quasistationary circulation in the equatorial latitudes is also intensified.]

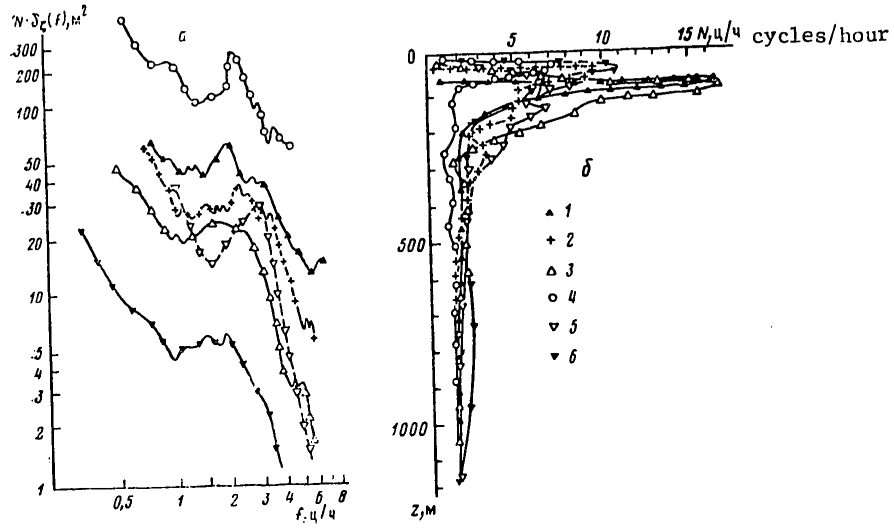

Fig. 2. a) High-frequency ranges of spectra of rises of the thermocline in different regions; b) profiles of Väisälä frequency: 1) North African basin, 2) Hydrophysical polygon, 3) Bay of Bengal, 4) Iberian basin, 5) Seychelles region, 6) Sargasso Sea

A change in the total energy of internal waves with a change in the width of the frequency range of their existence appears extremely probable, as is the retention of the level of the high-frequency part of the spectrum of internal waves with a decrease in f_i, which resembles the nondependence of the equilibrium part of the spectrum of wind waves on wind force and the position of the spectral maximum. The nature of the "equilibrium character" of the high-frequency part of the spectrum of internal waves remains unclear. This can indicate, for example, some limiting, saturated state of the corresponding spectral components, as occurs in wind waves.

Another characteristic property of the experimental spectra is that in the high-frequency region their attenuation does not conform to the general law. Here the energy of these spectra is increased, which is manifested in the form of individual peaks or plateaus. Figure 2,a shows the high-frequency parts of the spectra measured in different regions of the Atlantic and Indian Oceans and relating to the upper horizons, where, as a rule, these peaks were most clearly expressed. The measurements were made with both distributed and point anchored temperature

sensors. Figure 2,b shows the profiles of the Väisälä frequency N(z) for all the considered regions. The following pattern can be seen in the analysis of these two figures: the frequencies of the peaks falling in the range 1.5-3 cycles·hour^{-1} fall closer to the frequencies N_b at which there is a sharp broadening of the waveguide in the thermocline than to the local Väisälä frequencies. In actuality, the local Väisälä frequencies for the considered measurements were from 4 to 13 cycles·hour^{-1} and exceeded the frequency of the peaks by a factor of 2-6. At the same time, all the observed N(z) curves have the following common characteristic: a more or less narrow peak of the Väisälä frequency corresponding to the waveguide in the upper thermocline (depths from 10 to 100-200 m); with an increase in depth there is a rather sharp replacement by layers with a slow change of N(z) and the frequency of this sharp transition from the peak to quasiconstant values of the Väisälä frequency N_b in all the considered cases is in the range from 1 to 2 cycles·hour^{-1}, that is, only a little below the frequency of the spectral peaks.

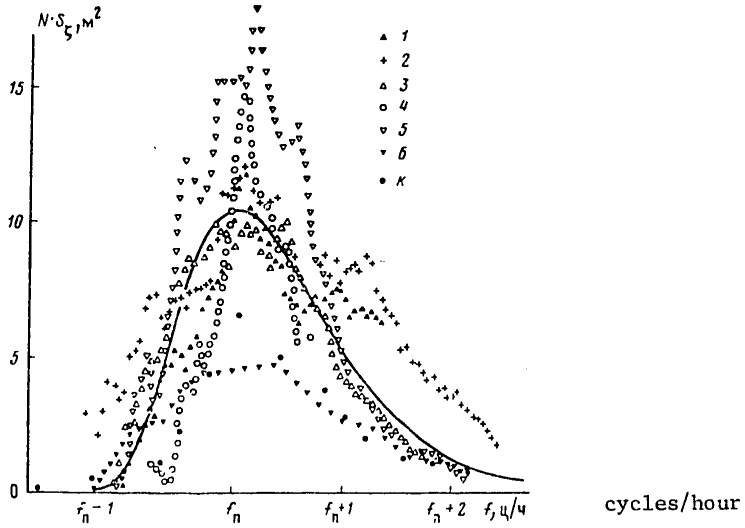

Fig. 3. High-frequency peaks of spectra of internal waves. For notations see Fig. 2; K designates the California region.

The reasons for the appearance of the high-frequency peaks are not entirely clear. The considerable differences in the frequency of the peaks from the local Väisälä frequency, and also the virtually single-mode structure of the short-period internal waves [7, 8], do not correspond to concepts on the formation of the high-frequency peaks due to the addition of many modes near the boundary of the waveguide [9] and therefore such a purely kinematic explanation is scarcely justified, at least under the conditions of the upper thermocline.

A direct identification of the observed waves with Kelvin-Helmholtz shear instability waves, as was done, for example, in [10], is impeded by the fact that short-period internal waves are propagated relative to the medium with a considerable phase velocity (close to the theoretical value for the first mode) [7], whereas Kelvin-Helmholtz waves are virtually motionless [11].

It can be postulated that the appearance of a peak near the frequency of a sharp broadening of the waveguide N_b is attributable to some quasiresonance properties of the thermocline examined in [12, 13] or the processes of absorption and scattering of waves in the deep layers of the ocean (the O. M. Phillips hypothesis, expressed at the Soviet-American Symposium on Internal Waves which was held in Novosibirsk in 1976 [14]). Finally, it can be assumed that the sporadically appearing short-period internal waves are radiated by wave-eddy turbulence of the upper quasihomogeneous layer of the ocean with the appearance of critical velocity shears there [15] or arise as a result of nonlinear decay of longer waves.

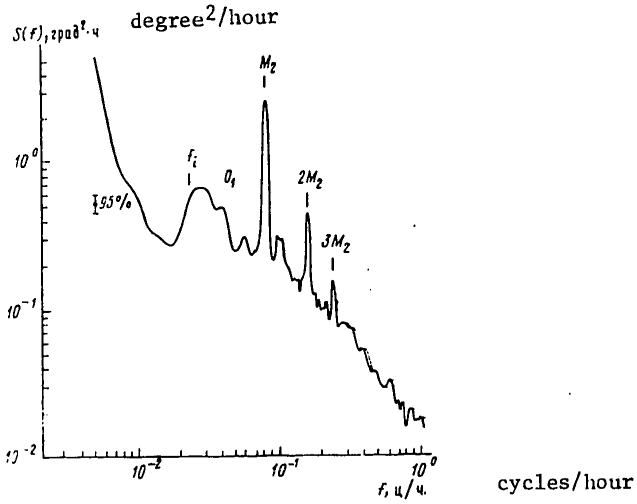

Fig. 4. Spectrum of temperature fluctuations in hydrophysical polygon of 1970: f_i is the inertial frequency, O_1 is the solar diurnal period, M_2 is the lunar semidiurnal period, $2M_2$, $3M_2$ are harmonics of the lunar period.

Due to Doppler distortions associated with the mean transfer of water relative to fixed instruments, the measured frequency can differ substantially from the true frequency, by which we will understand the frequency of waves in a reckoning system moving together with the medium in which they are propagating. Therefore, without attempting to establish any more definite relationships between the measured frequencies of the peaks and the Väisälä frequency, we note that the mean frequency of all the peaks f_p = 2 cycles·hour^{-1} is very close to the frequency of the sharp broadening of the waveguide N_b = 1-2 cycles·hour^{-1} in all the described observation regions, as should be observed in the case of resonance properties of the

thermocline [12, 13] or the influence of wave absorption in the spirit of the Phillips hypothesis.

Now we will attempt to discriminate the high-frequency peaks, excluding the background part of the spectrum. We will assume that the differences in the absolute spectral levels of the high-frequency parts of the spectra which are shown in Fig. 2,a were caused by errors in determining the vertical temperature gradients T_z' used for conversion of the temperature spectra $S_T(f)$ into vertical displacement spectra $S_\zeta(f) = (T_z')^{-2} S_T(f)$. If the values determined by expression (2) are used as the true values of the spectral background above which the high-frequency peaks rise, we obtain the following formula for computing the corrected spectral ordinates of the peaks themselves:

[п = peak]

$$NS_\zeta^{\text{п}}(f) = qS_\zeta(f) - C_1 f^{-2}. \tag{5}$$

The correction factor q is determined at the point f_0, directly preceding the high-frequency peak, where the decrease of the spectrum with frequency ceases: $q = C_1 f_0^{-2} S_\zeta^{-1}(f_0)$. In the case of measurements with distributed sensors, making possible a more precise evaluation of the vertical displacements, the correction factor was not introduced and the ordinates of the peaks were determined directly as rises above the measured background.

Figure 3 shows all the peaks discriminated in this way, which also were matched in frequency. Here also as a comparison we have plotted a peak measured by Pinkel near California [8, Fig. 7] and denoted by the letter k. The spectrum was evaluated directly from the vertical displacements of the isotherms; its frequency was 3.5 cycles·hour^{-1}. In this same figure we have plotted a curve more or less satisfactorily approximating the high-frequency peaks:

$$\hat{N}S_\zeta^{\text{п}}(\hat{f}) = C_{\text{п}}(\hat{f} - \hat{f}_0)^4 \exp[-3(\hat{f} - \hat{f}_0)], \tag{6}$$

where "^" denotes normalization to a frequency 1 cycle·hour^{-1}, C_p = 180 m^2 and $\hat{f}_0$ = 0.7. In this case the frequency of the peak is equal to its mean value 2 cycles·hour^{-1}.

However, it is easy to obtain the dispersion of the vertical displacements of the thermocline caused by short-period internal waves:

$$\overline{\zeta^2} = \int_{\hat{f}_*}^{\hat{N}} S_\zeta^{\text{п}}(\hat{f})\, d\hat{f} = 0{,}1 C_{\text{п}} / N. \tag{7}$$

With a typical value C_p = 180 m^2 this gives the mean square amplitude $\zeta \approx 4.2/\sqrt{N}$, m.

The greatest differences from the curve are observed in the Seychelles and Sargasso polygons, and also near California. These three spectra, in contrast to the others, correspond to relatively brief measurements (8 hours for California, 6 hours for the Sargasso Sea and 17 hours for the Seychelles polygon). However, only the Seychelles peak, evidently, would approach to the approximating curve, measuring over a long time interval, since already in the next 17-hour segment of the measurements this peak is not manifested. The small height of the peaks measured near the shores of California and in the Sargasso Sea probably corresponds to a lesser

amplitude of the short-period waves than in other regions because the spectrum of the adjacent segment of measurements in the Sargasso Sea does not contain a peak and the heights of the peaks obtained by Pinkel from the longer records (see [8]) are even less significant.

Thus, the approximation of internal waves (6) which we obtained can make no pretense to broad representativeness and is not so much a universal as a typical form of this spectrum. By varying the values of the coefficient C_p and the frequency position of the peak, possibly associated with the frequency of the sharp broadening of the waveguide, it is possible to achieve a better description of the peak in each specific case. Nevertheless, the small number of reliable measurements for the time being still does not make it possible to draw any conclusions concerning the geographical variability of the peak. However, some ideas can be expressed concerning the temporal variability of the peak on the basis of data on the intermittence of short-period internal waves [16]. Assuming that the ratio of the local time of existence of the short-period internal waves to the entire sufficiently great observation time is 1:3 with mean $C_p = 180$ m^2, we find that C_p varies from zero in the absence of trains of high-frequency internal waves to 540 m^2 within such chains. This corresponds to a change in the mean square amplitude of internal waves from 0 to $\zeta = 3$ m, with a typical value $N = 6$ cycles·hour^{-1}.

One of the invariable characteristics of the frequency spectra of internal waves in the ocean is a peak corresponding to tidal fluctuations. The amplitude of this peak is subject to sharp changes in time and space, which can be attributed to the great role of local topography of the bottom and hydrological conditions [17].

A reliable and representative illustration of ocean internal tides is the observations of the well-expressed narrow-band semidiurnal temperature fluctuations in the Hydrophysical Polygon of 1970 in the Atlantic. Figure 4 shows the spectrum of temperature fluctuations at the 200-m horizon of this polygon, computed on the basis of all available observations for a six-month period using a photothermograph with a high resolution $\Delta f_0 = 0.0025$ cycle·hour^{-1} and a number of degrees of freedom of about 200. The narrow and high peak of semidiurnal fluctuations, having a maximum in the period of the lunar semidiurnal tide $\tau_{M_2} = 12.4$ hours, contains about 13% of the total dispersion of the temperature fluctuations. The ratio of the central frequency ($f_{M_2} = 0.08$ cycle·hour^{-1}) to the width of the peak near its base ($\Delta f = 0.02$ cycle·hour^{-1}) is 4, which indicates the narrow-band character of the tidal fluctuations. Figure 4 shows the second and third harmonics of the semidiurnal fluctuation and the peak near the inertial frequency, which may be a consequence not so much of vertical, but instead, horizontal displacements in the inertial waves in the presence of horizontal temperature gradients in the thermocline, where they play a significant role.

In summarizing, the following conclusions can be drawn concerning the structure of the frequency spectra of internal waves in the upper layer of the ocean. The frequency spectra of the vertical displacements of the thermocline consist of a background part, decreasing monotonically with frequency, over which rise narrow and high peaks of tidal (primarily semidiurnal) fluctuations and broader peaks of short-period internal waves (with frequencies from 1 to several cycles per hour). The background part is satisfactorily described by the Garrett-Munk model with

some correction (2) relating to dependence on geographical latitude.

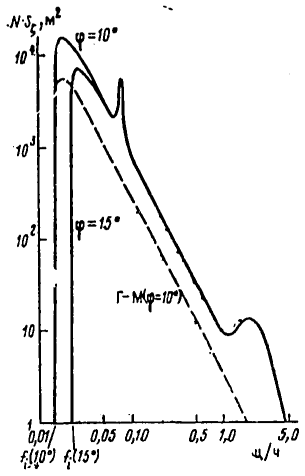

cycles/hour

Fig. 5. Generalized frequency spectrum of vertical displacements of the thermocline in internal waves for different geographical latitudes φ. The broken line corresponds to the Garrett-Munk model for φ= 10°; the solid curves correspond to a modified model for φ = 10 and 15°.

Short-period internal waves are essentially nonstationary in time and nonuniform in space. They are manifested in the form of chains of relatively narrow-band fluctuations intermittent with sectors of more random and less intense "background" fluctuations. The duration of the trains is some hours; the intermittence of the trains, that is, the ratio of the total time of their existence to the entire time of the observations, is usually characterized by a few tens of percent. The height of the waves within the trains can attain 10 m or more, which is close to the typical height of the semidiurnal waves in the thermocline.

Figure 5 shows the generalized frequency spectrum of rises of the thermocline in internal waves, conveying all the above-mentioned characteristics of such a spectrum -- nondependence of the high-frequency part on geographical latitude, the existence of semidiurnal and high-frequency peaks. Here also the dashed line represents the Garrett-Munk spectrum (1) for a latitude of 10°; the solid curves represent the spectra (2) for latitudes 10 and 15°. The difference in latitudes is reflected only in the lowest-frequency part of the spectra. The width and height of the peaks, as well as the position of the high-frequency maximum, can vary in dependence on the place and time of the measurements. The figure corresponds to some typical values in the upper thermocline in the ocean. The typical values of the mean square vertical displacements of the upper thermocline ζ in the short-period, tidal and background internal waves are related as 1:2:3; the absolute values of the corresponding amplitudes can be evaluated approximately using the

product $\zeta\sqrt{N} \approx 4$; 8 and 13 m·hour$^{-0.5}$. (The values for the background part correspond to the subtropical latitudes.)

In conclusion we emphasize that the small number of observations at our disposal, generally speaking, does not make it possible to draw reliable conclusions concerning the change in the spectrum of internal waves with latitude. We attempted to tie in the great difference in the energy of waves in the Sargasso Sea and two equatorial regions of the Indian Ocean with the great difference in geographical latitudes, although it is also impossible to preclude the influence of any other local factors, such as bottom topography, currents, etc. In this connection the proposed modification of the Garrett-Munk model with respect to the dependence on inertial frequency has a preliminary character and requires checking, which can be accomplished within the framework of a further study of the geography of internal waves in the world ocean.

BIBLIOGRAPHY

1. Garrett, C., Munk, W., "Space-Time Scales of Internal Waves," GEOPHYS. FLUID DYN., Vol 3, No 3, 1972.

2. Garrett, C., Munk, W., "Space-Time Scales of Internal Waves. A Progress Report," J. GEOPHYS. RES., Vol 80, No 3, 1975.

3. Sabinin, K. D., Serikov, A. N., Shulepov, V. A., "Frequency Spectra of Internal Waves," VOPROSY SUDOSTROYENIYA. AKUSTIKA (Problems in Shipbuilding. Acoustics), No 2, 1978.

4. Sabinin, K. D., "Use of Distributed Temperature Sensors for Measuring Internal Waves," POVERKHNOSTNYYE I VNUTRENNIYE VOLNY (Surface and Internal Waves), Izd. MGI AN UkrSSR, Sevastopol', 1978.

5. Sabinin, K. D., Serikov, A. N., "Spatial-Temporal Parameters of Short-Period Internal Waves in the Indian Ocean," GIDROFIZICHESKIYE I OPTICHESKIYE ISSLEDOVANIYA V INDIYSKOM OKEANE (Hydrophysical and Optical Investigations in the Indian Ocean), Moscow, "Nauka," 1975.

6. Monin, A. S., Kamenkovich, V. M., Kort, V. G., IZMENCHIVOST' MIROVOGO OKEANA (Variability of the World Ocean), Leningrad, Gidrometeoizdat, 1974.

7. Brekhovskikh, L. M., Konjaev, K. V., Sabinin, K. D., Serikov, A. N., "Short-Period Internal Waves in the Sea," J. GEOPHYS. RES., Vol 80, No 6, 1975.

8. Pinkel, R., "Upper Ocean Internal Wave Observations from FLIP," J. GEOPHYS. RES., Vol 80, No 27, 1975.

9. Desaubies, Y. J. F., "A Linear Theory of Internal Wave Spectra and Coherence Near the Väisälä Frequency," J. GEOPHYS. RES., Vol 80, No 6, 1975.

10. Korotayev, G. K., Panteleyev, N. A., "Experimental Investigations of Hydrodynamic Instability in the Ocean," OKEANOLOGIYA (Oceanology), Vol 17, No 6, 1977.

11. Terner, Dzh., EFFEKTY PLAVUCHESTI V ZHIDKOSTYAKH (Buoyancy Effects in Fluids), Moscow, "Mir," 1977.

12. Sabinin, K. D., "Correlation of Short-Period Internal Waves With the Vertical Density Gradient in the Sea," IZV. AN SSSR, FAO (News of the USSR Academy of Sciences: Physics of the Atmosphere and Ocean), Vol 2, No 8, 1966.

13. Kase, R. H., Clarke, R. A., "High-Frequency Internal Waves in the Upper Thermocline During GATE," DEEP SEA RES., Vol 25, No 9, 1978.

14. Miropol'skiy, Yu. Z., Sabinin, K. D., "Soviet-American Symposium on Internal Waves in the Ocean," OKEANOLOGIYA (Oceanology), Vol 17, No 2, 1977.

15. Sabinin, K. D., Serikov, A. N., "Characteristics of the Spatial Spectrum of Short-Period Internal Waves in the Ocean," OKEANOLOGIYA, Vol 16, No 5, 1976.

16. Sabinin, K. D., "Some Characteristics of Short-Period Internal Waves in the Ocean," IZV. AN SSSR, FAO, Vol 9, No 1, 1973.

17. Lyashenko, A. F., Sabinin, K. D., "Spatial Structure of Internal Tides in the Hydrophysical Polygon of 1970 in the Atlantic," IZV. AN SSSR, FAO, Vol 15, No 8, 1979.

5303
CSO: 1865/85

UDC 550.834.087.4:528.47.629.472

ANALOG REGISTRY AND PROCESSING OF ECHO SIGNALS IN MAPPING OF THE SHELF

Moscow GEODEZIYA I KARTOGRAFIYA in Russian No 12, Dec 80 pp 39-43

[Article by A. I. Svechnikov and Ye. V. Brener]

[Text] The use of acoustic research methods for solving problems in the mapping of bottom deposits on the shelf is determined by the following principal factors:
-- high productivity of the survey due to the continuity of the process of acoustic measurements during movement of the ship;
-- possibility of carrying out a continuous areal survey with the use of side-view sonars;
-- possibility for obtaining information not only on the depth of the water body, but also on the nature of the bottom deposits.

The active echosounding method is the basis for the acoustic research method. As a result of interaction between an acoustic sounding pulse and the object of the investigation an echo signal is formed which carries information both on the distance to the object, but also on its properties [3].

The registry of echo signals arising during the interaction of acoustic radiation with bottom sediments on the paper tape of an automatic recorder creates only the prerequisites, shows the possibility for the extraction of information from the echo signal not only on the fact of reflection, but also on the nature of the bottom deposits, their lithological composition.

Bottom deposits of different lithological type have definite differences in physicomechanical properties [6]. They lead to changes in the echo signal and can be manifested in the character of the echogram. For example, with a contrasting transition from acoustically soft to acoustically hard sediments. Only under these conditions can a visual interpretation of the echograms obtained on paper tape give good results [2].

It is obvious that only a changeover from a visual, qualitative interpretation to the measurement of the principal characteristics of an echo signal and on this basis, revelation of the regular correlation between the nature of changes in the echo signal and specific lithological types of bottom deposits, can facilitate the improvement of remote diagnosis methods.

The measurement and computation of the characteristics of echo signals is possible both in the registry process and in the interpretation process. For the processing of data from acoustic investigations in the interpretation stage it is necessary to

register the echo signals on a carrier which will ensure the possibility of repeated reproduction of the registered signals with minimum distortions with respect to echo signals registered in the course of the survey.

We will examine the possibilities of using an analog magnetic record for the registry and prolonged storage of echo signals.

Among the fundamental premises which determine the possibility of using an analog magnetic record are the following:
-- the possibility of the registry of acoustic information at a real time scale;
-- relative simplicity in the registry of large volumes of data;
-- the possibility of multiple reproduction of the magnetic records, which makes possible the use of a whole set of processing procedures in the interpretation process.

The use of two-channel analog registry, in addition, makes it possible to register additional service information.

In the mapping of bottom deposits on the shelf by acoustic methods it is necessary to solve two fundamental problems -- determine the depth of the bottom deposits and the nature, lithological type of sediment. The first problem involves the registry of the propagation of an echo signal from the bottom surface. It is obvious that the registry accuracy will be determined both by the geometrical measurement errors characterizing the sounding pulse and the accuracy in registering the time intervals on a magnetic tape, which for the most part is dependent on fluctuations in the rate of the magnetic tape relative to the recording and reproducing heads [1]. Fluctuations of the rate of the magnetic tape usually are evaluated using the coefficient of rate fluctuation or the detonation coefficient [5]. For example, with the registry on a magnetic tape of the time intervals related to depth measurements in a range up to 200 m with an absolute error of 20-40 cm, the detonation coefficient for the magnetic recorder must not be greater than 0.1%.

In the remote determination of the lithological type of bottom sediment the emphasis is on the depth of penetration of acoustic radiation into the sediments and the changes arising in the echo signal during their interaction. The reflected echo signal carries information on the lithological type of sediment and therefore the accuracy in registry of the echo signal on the magnetic tape should ensure a reliable separation of the bottom deposits on the basis of the measured characteristics of the echo signal. For example, the maximum value of the echo signal envelope determines such an important characteristic of bottom sediments as the reflection coefficient. According to the data in [6], the reflection coefficients for sandy deposits fall in the range 0.41-0.37, for sandy-clayey deposits -- 0.32-0.21, for clayey deposits -- 0.25-0.17 and for silty deposits -- 0.16 or less. Accordingly, for reliable separation of bottom sediments into four major lithological groups the accuracy in the registry of the amplitude value of the echo signal must not be less than 10%.

Thus, assurance of the necessary accuracy in the registry of time intervals and reliable reproduction of the registered amplitude values of the echosignals is possible when as the magnetic recorder for the registry of acoustic information use is

made of specialized apparatus for precise magnetic recording or special measuring magnetic recorders.

Among the different types of Soviet apparatus for precise magnetic recording it is possible to employ the MEZ-74 two-channel magnetic recorder [4].

Among foreign analog magnetic recorders for this purpose it is possible to use a "B & K" (Denmark) magnetic recorder type 7001, which is a two-channel recording instrument with a frequency range 0-20 KHz, with a linearity of more than 1%, with distortions not greater than 1.5% and integral vibrations of about 0.1-0.15%/

It should be noted that determination of depth in the water with a sufficiently high accuracy is possible when using acoustic emitters with a radiation frequency of about 50-150 KHz, whereas for solution of problems in the classification of bottom sediments it is necessary to use radiation frequencies of about 1-7 KHz.

Two-channel magnetic analog registry makes possible rather simple solution of the problem of registry and storage of information received in the survey process from high- and low-frequency emitting systems.

Figure 1 is a block diagram of apparatus for carrying out work for the mapping of bottom deposits with the use of a two-channel analog magnetic recorder.

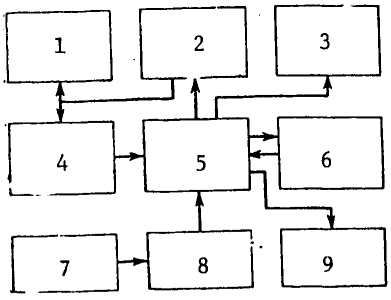

Fig. 1.

KEY:
1) Low-frequency emitter
2) Generator for excitation of acoustic systems
3) Express-recorder
4) High-frequency receiver-emitter
5) Control unit
6) Two-channel magnetic recorder
7) Receiver
8) Measuring amplifier
9) Curve plotter

The outfit includes a high-frequency receiving-emitting system with a working frequency of 140 KHz, a low-frequency emitting system with a maximum of the emission spectrum at a frequency of 4 KHz, a generator for the excitation of the acoustic systems, a receiver, measuring amplifier, two-channel analog magnetic recorder, express information recorder, curve plotter and control unit.

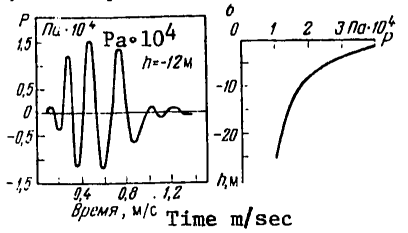

Fig. 2.

Figure 2 shows the shape of the pulse generated by the low-frequency emitting system and a curve of the change in peak pressure developed by the emitter with depth with an excitation voltage of 2 KV. Measurements of peak pressure were made using a spherical hydrophone with a response of 10 μV/bar.

The generator for the excitation of acoustic systems produces voltage pulses with a frequency of 1 Hz with a capacitance of the reservoir capacitors of 100 μF and a voltage 100-10 000 V. The echo signal amplifier used was a U2-7 measuring amplifier with a frequency range 0-20 KHz and a nonuniformity of the frequency characteristic less than 0.3 db with an amplification factor 10-80 db. The receiver response is 10 V/bar. The registry of the echogram is on electrothermal paper on an express-information recorder of the "Paltus-M" type. Simultaneously with registry of the echogram there is registry of echo signals on magnetic tape of a two-channel magnetic recorder with the frequency range 31.5 Hz-16 KHz, a detonation coefficient of 0.07% and harmonic distortions of less than 1.5%. The registry of the echo signal characteristics after processing is accomplished using a two-coordinate plane table curve plotter of the PDP-4 type.

Figure 3 is a block diagram of the control circuit. The system ensures the registry of information directly during the course of acoustic investigations, the reproduction and analog processing of survey materials.

In a regime with registry of the synchronization pulse a timer produces a synchronization signal which is fed for registry in the first track; this determines the moment of onset of registry. In addition, the timer feeds a signal to the circuit for blocking the receiving channel of the outfit, thereby ensuring protection of the reception channels from an overload when generating a sounding pulse. Then 1 msec after the synchronization pulse, a pulse is fed for triggering the generator for the excitation of acoustic systems. A high-frequency echo signal passes through the blocking circuit to the shaping circuit. There it is converted into a rectangular pulse with an amplitude of about 0.5 V and a duration of 100 μsec and this is fed to an amplifier for registry of the reading "bottom" in the first track of the magnetic recorder.

The low-frequency echo signals reflected from the sedimentary layers are fed to a measuring amplifier through a blocking circuit which forbids the passage of echo signals in definite registry limits controlled by a timer. By means of the timer it is possible to carry out both manual setting of the registry limits and automatic tracking of the stipulated time interval of registry in the limits (0.1-100 msec). Low-frequency noise is suppressed by an active high-frequency filter with a cutoff steepness 40 db per octave at a cutoff frequency 1000 Hz.

After time selection and frequency limitation the echo signals are fed to an amplifier for registry in the second channel of the magnetic recorder.

In the reproduction of the magnetic record the control circuit ensures three regimes of analog processing and registry of the recorded information. This includes the construction of the vertical profile of depth in the water, curves of change of the reflection coefficient and the integral characteristic curve of the echo signal.

In the regime for construction of the vertical profile from the "depth measurement" signal there is triggering of the depth integrator, which transforms the time into a voltage in conformity to a linear law. Using the "bottom reading" signal the circuit for shaping the control signals stops the depth integrator and transmits the state of the integrator to the circuit for storage of the sample, which stores the depth value to the next cycle of measurements. After transmitting a particular depth value the depth integrator is discharged.

The acoustic stiffness of the bottom sediments is determined using the circuit for measurement of the reflection coefficient, which consists of a time automatic volume control (TAVC) and a peak detector.

A low-frequency echo signal in a reproduction regime is fed through a blocking circuit to the TAVC circuit and then to a peak detector, where there is determination of the amplitude value of the envelope of an echo signal, discriminated from the totality of the echo signals. This includes a blocking circuit and a circuit for the shaping of control signals.

In the regime for computing the integral characteristic curves the echo signals from the TAVC are fed to an integrator with an integration time constant of 100 msec. Here the positive half-waves of the echo signal are integrated in stipulated registry limits. Then the state of the peak detector or the integrator is fed to the circuit for storage of the sample and from there, through a LF filter (LFF), it is fed to the amplifier of the curve plotter "U" coordinate.

The results of processing of analog magnetic records, obtained when carrying out acoustic investigations along profile No 26 of the experimental lithological polygon, are presented in Fig. 4. The figure also shows an echogram and geological section constructed using drilling data. The curves of change of the reflection coefficient along the profile were normalized using the maximum value of the envelope of the sounding pulse, whereas the integral characteristic curves were normalized using the value of the integral determined for positive half-waves of the sounding pulse.

On the curve of changes of the reflection coefficient it is possible to discriminate regions with increased values of the reflection coefficient (0.4-0.45) characteristic of sandy-gravelly deposits, for example, in the region of points 1 and 2, and also regions with values of the reflection coefficient 0.15-0.2, characteristic for silty-clayey deposits. For fine and pulverized sands the values of the reflection coefficients fall in the range 0.25-0.3.

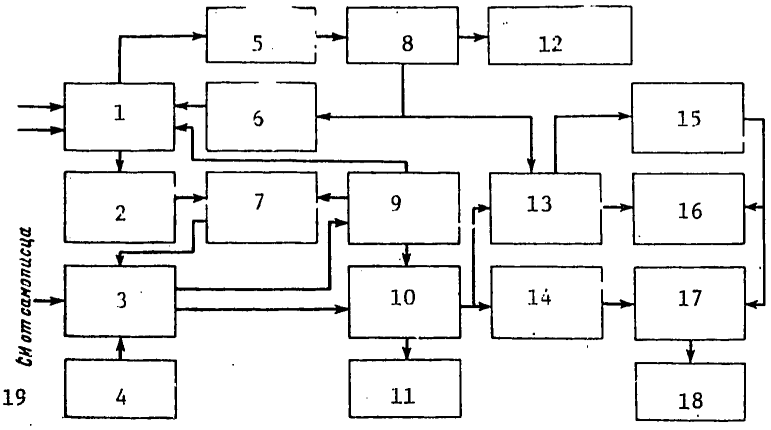

KEY:

1. Blocking circuit
2. Shaper
3. Synchronization circuit
4. Synchronization generator
5. Measuring amplifier
6. Amplifier for registry and reproduction in 2d track
7. Amplifier for registry and reproduction in 1st track
8. High-frequency filter
9. Timer
10. Circuit for shaping control signals
11. Horizontal scanning circuit
12. Express recorder amplifier
13. TAVC circuit
14. Depth integrator
15. Peak detector
16. Integrator
17. Storage circuit
18. Low-frequency circuit
19. Stabilizing pulse from automatic recorder

It should be noted that in the sectors of the profile lying to the left and right of point 3 there are reduced values of the reflection coefficient, evidence of the development of silty-clayey deposits in these sectors.

Thus, the determined distribution of the coefficients makes it possible to determine the geological section more precisely and increase the reliability of determination of the lithological type of sediment.

The integral characteristics of echo signals along the profile were obtained for the two intervals 0-2 msec and 2-36 msec. The appearance of the first echo signals was used as the beginning of the reading. The changes in the integral characteristic curve obtained for an integration time of the order of a prolonged sounding pulse coincide with the changes in the reflection coefficient. The integral characteristics for the second interval give some idea concerning the intensity of the

echo signals received from the lower-lying layers or arising as a result of multiple reflections. For example, in places of clayey deposits there are increased values of the integral characteristic curve; for sands of medium grain size their values are greater in comparison with fine-grained sands due to a change in the intensity of the multiple wave.

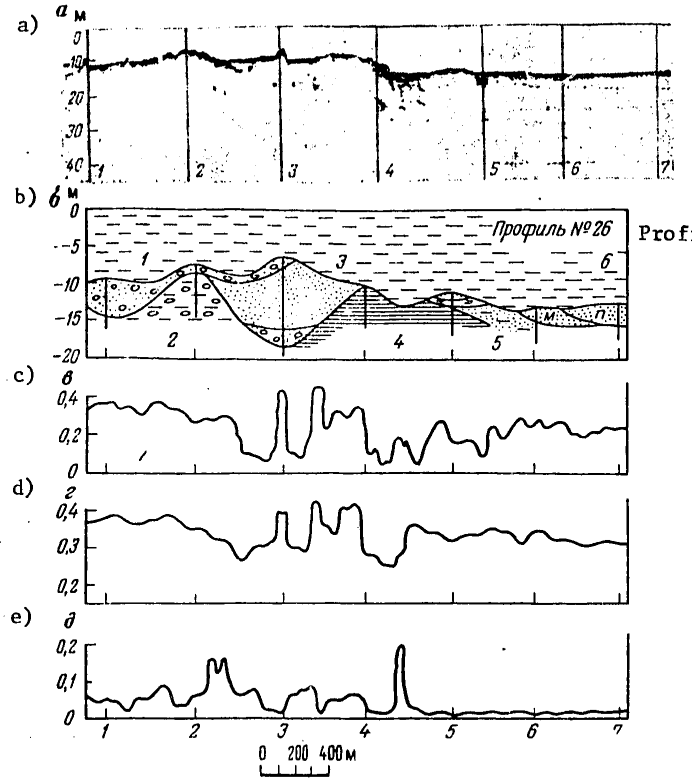

Profile No 26

Fig. 4. Results of analog processing of magnetic records: 1) gravelly-pebbly deposits; 2) morainal deposits; 3) sands with medium grain size; 4) varved clays; 5) fine sands, pulverized; 6) sandy loams

In conclusion it should be noted that the use of analog magnetic recording in the solution of mapping problems on the shelf ensures registry and storage of great volumes of acoustic information, creates prerequisites for the analog processing of echo signals and affords a possibility of obtaining data for identification of bottom deposits not only on the basis of records of echograms, but with allowance for such objective data as the impedance and integral characteristics of bottom sediments.

In addition, analog magnetic recording makes possible rather simple changeover to the digital processing of acoustic information with the use of highly productive digital computers using devices for the input of analog information, which to a considerable degree will broaden the range of procedures and processing methods and will facilitate a changeover to the automated processing of the results of acoustic investigations on the shelf.

Without question, digital registry of the results of acoustic measurements at a real time scale has indisputable advantages both with respect to the accuracy of registry and convenience in the exchange of information with the digital computer, but the great velocity of receipt of acoustic information (100-200 kbyte/sec) and its considerable volumes (15-20 kbyte/sec) create definite difficulties in the development and creation of digital magnetic recorders of hydroacoustic information.

BIBLIOGRAPHY

1. Aksenov, V. A., Viches, A. I., Gitlits, M. V., TOCHNAYA MAGNITNAYA ZAPIS' (Precise Magnetic Recording), Moscow, Energiya, 1973.

2. Muzylev, V. S., Svechnikov, A. I., "Use of Acoustic Sounding for Lithological Mapping of Bottom Deposits," GEOFIZICHESKIYE ISSLEDOVANIYA PRI RESHENII STRUKTURNYKH I POISKO-RAZVEDOCHNYKH ZADACH (Geophysical Investigations for Solving Structural and Reconnaissance-Exploration Problems), Leningrad, ZAPISKI LGI im. G. V. PLEKHANOVA (Notes of Leningrad Geological Institute imeni G. V. Plekhanov), Vol XIX, No 2, 1976.

3. Nigul, U. K., EKHO-SIGNALY OT UPRUGIKH OB"YEKTOV (Echo Signals From Elastic Objects), Tallin, Valgus, 1976.

4. Rokotov, S. P., Titov, M. S., OBRABOTKA GIDROAKUSTICHESKOY INFORMATSII NA SUDOVYKH TsVM (Processing of Hydroacoustic Information on Shipboard Digital Computers), Leningrad, Sudostroyeniye, 1979.

5. Travnikov, Ye. N., MEKHANIZMY APPARATURY MAGNITNOY ZAPISI (Mechanisms of Magnetic Recording Equipment), Kiev, Tekhnika, 1976.

6. Hampton, L., AKUSTIKA MORSKIKH OSADKOV (Acoustics of Sea Sediments), Moscow, Mir, 1977.

5303
CSO: 1865/108

UDC 532.58

EMISSION OF INTERNAL WAVES FROM RAPIDLY MOVING SOURCES IN AN EXPONENTIALLY STRATIFIED FLUID

Moscow DOKLADY AKADEMII NAUK SSSR in Russian Vol 256, No 6, 1980 pp 1375-1378

[Article by V. A. Gorodtsov, Institute of Mechanical Problems USSR Academy of Sciences, manuscript submitted 30 Jun 80]

[Text] Computations of the field of internal waves in a density-stratified fluid generated by moving bodies are considerably simplified if one knows the volumetric or surface sources equivalent to the bodies in their hydrodynamic effect. The finding of such sources is a difficult problem, in a general case soluble approximately or numerically. However, for great velocities of movement the integral characteristics of the wave field are slightly dependent on the specific form of the sources and universal asymptotic dependences are correct.

Small perturbations of the field of pressure p in an exponentially stratified (case of a constant Väisälä-Brent frequency N) ideal incompressible fluid, caused by a mass source m(r,t), in the Boussinesq approximation are described by the equation [1,2]

$$\left[\left(\frac{\partial^2}{\partial t^2}+N^2\right)\left(\frac{\partial^2}{\partial x^2}+\frac{\partial^2}{\partial y^2}\right)+\frac{\partial^4}{\partial t^2\partial z^2}\right]p=-\left(\frac{\partial^2}{\partial t^2}+N^2\right)\frac{\partial}{\partial t}m\rho_0. \tag{1}$$

Here t is time, x, y, z are the horizontal and vertical coordinates, ρ_0 is the density of the fluid in an unperturbed state, assumed henceforth to be constant.

For a uniformly moving source $m(r, t) = m_0 f(r - v_0 t)$ the energy of emission of internal waves per unit time is equal to the value

$$W=\int d^3r\,p(r,t)m(r,t). \tag{2}$$

Due to the linear homogoneous correlation (1) between p and m it is possible to give W a form of expression which is quadratic relative to the amplitude of the source. Using the Fourier transform for the variables r, t, from (1), (2) we obtain

$$W=\frac{\rho_0 m_0^2}{8\pi^3}\int d^3k\,d\omega\,|\omega|(N^2-\omega^2)\delta(\omega-\mathbf{kv}_0)\delta(L)/f(\mathbf{k})|^2,$$

$$L\equiv\omega^2k_z^2-(N^2-\omega^2)(k_x^2+k_y^2).$$

Here $k = (k_x, k_y, k_z)$, ω are Fourier variables conjugate to the variables $r = (x, y, z)$, t, and $\delta(x)$ is the Dirac delta function.

This formula can also be rewritten in another convenient form

$$W = \rho_0 m_0^2 \int d^3r\, d^3r' f(\mathbf{r}) f(\mathbf{r}') w(\mathbf{r} - \mathbf{r}'), \tag{3}$$

$$w(\mathbf{r}) = \frac{1}{8\pi^3} \int d^3k d\omega |\omega| (N^2 - \omega^2) \delta(\omega - \mathbf{k}\mathbf{v}_0) \delta(k_z) e^{i\mathbf{k}\mathbf{r}}. \tag{4}$$

As a simplification we will limit ourselves to the cases of horizontal and vertical moving sources. In the second case after performing integrations for the components of the wave vector k we obtain a representation of w(r) in the form of a single integral of the Bessel function

$$w(\mathbf{r}) = \frac{1}{4\pi v_0} \int_0^N d\omega\ \omega \cos\left(\frac{\omega z}{v_0}\right) J_0\left(\frac{\omega}{v_0}\sqrt{x^2 + y^2}\sqrt{N^2 - \omega^2}\right). \tag{5}$$

for which, in the case of great velocities ($v_0 \to \infty$) an asymptotic expansion is correct ($\ln\gamma$ is the Euler constant)

$$\frac{8\pi v_0}{N^2} w(\mathbf{r}) \approx 1 - \left(\frac{Nz}{2v_0}\right)^2 - \frac{N^2(x^2 + y^2)}{2v_0^2}\left(\ln \frac{2v_0}{\gamma N\sqrt{x^2 + y^2}} + \frac{1}{4}\right) + \ldots$$

In accordance with this expansion and the general formula (3), for the energy losses of a vertically moving source at great velocities we will have the asymptotic formula

$$W \approx \frac{\rho_0 m_0^2 N^2}{8\pi v_0} \left|\int d^3r f(\mathbf{r})\right|^2. \tag{6}$$

if the integral entering into it does not becomes equal to zero. Otherwise, when there is a compensation of the "receipts" and "losses" it is necessary to keep the next terms of the expansion. For a source for which $\int dz f(\mathbf{r}) = 0$, $\int d^3r f(\mathbf{r}) z \neq 0$, we obtain

$$W \approx \frac{\rho_0 m_0^2 N^4}{16\pi v_0^3} \left|\int d^3r f(\mathbf{r}) z\right|^2. \tag{7}$$

Formulas (6) and (7) become precise in the case of a point source and a vertical doublet respectively; the integral factor in (6) is then equal to unity, but in (7) -- d^2/m_0^2 (d is the dipole moment of the doublet).

In the case of horizontal movement of the source, from formula (4) it is also possible to obtain a representation of the function w(r) through single integrals of the cylindrical functions:

$$\frac{2\pi^2 v_0}{N^2} w(\mathbf{r}) = \int_a^1 d\xi \sqrt{1 - \xi^2} \cos\left(\frac{Nx\xi}{v_0}\right) K_0\left(\frac{N\lambda}{v_0}\right) - \frac{\pi}{2} \int_0^a d\xi \sqrt{1 - \xi^2} \cos\left(\frac{Nx\xi}{v_0}\right) Y_0\left(\frac{N\lambda}{v_0}\right). \tag{8}$$

Here $a = |z|/\sqrt{y^2 + z^2}$, $\lambda = |\xi 2y^2 - (1 - \xi 2)|z2|1/2$. For large velocities of movement, using expansions of cylindrical functions and the cosine, we have

$$\frac{2\pi^2 v_0}{N^2} w(\mathbf{r}) \approx \int_0^1 d\xi \sqrt{1 - \xi^2} \left[\ln \frac{2v_0}{\gamma N\lambda} - \frac{N^2 x^2}{2v_0^2} \xi^2 \ln \frac{2v_0}{\gamma N\lambda} + \frac{N^2(y^2 + z^2)}{4v_0^2} (\xi^2 - a^2) \ln \frac{2v_0}{\gamma N\lambda} + \ldots\right]. \tag{9}$$

Hence follows an asymptotic formula for the energy loss per unit time by a source moving horizontally with a great velocity

$$W = \frac{\rho_0 m_0^2 N^2}{8\pi v_0}\left(A_1 \ln \frac{2v_0}{\gamma N} + B_1\right), \qquad (10)$$

$$B_1 = -\frac{4}{\pi}\int d^3r\,d^3r'\,f(\mathbf{r})f(\mathbf{r}')\int_0^1 d\xi\sqrt{1-\xi^2}\ln\Lambda,$$

$$A_1 = \left|\int d^3r f(\mathbf{r})\right|^2, \quad \Lambda = |\xi^2(y-y')^2 + (1-\xi^2)(z-z')^2|^{1/2},$$

if the total source $\int d^3rf(r)$ is different from zero. For a source of the type $\int dxf(r) = 0$, $\left|\int d^3rf(r)x\right|^2 \equiv A_2 \neq 0$ the following terms of expansion (9) become fundamental:

$$W = \frac{\rho_0 m_0^2 N^4}{32\pi v_0^3}\left(A_2 \ln \frac{2v_0}{\gamma N} + B_2\right), \qquad (11)$$

$$B_2 = -\frac{16}{\pi}\int d^3r\,d^3r'f(\mathbf{r})f(\mathbf{r}')xx'\int_0^1 d\xi\sqrt{1-\xi^2}\,\xi^2\ln\Lambda.$$

In the case of horizontal movement the simplest example of a point source loses sense, since here, in contrast to the case of vertical movement w(0) is not a finite value (compare (5), (8)).

As can be seen from the written formulas (6), (7), (10), (11), the coefficients of the higher terms of the expansions W for the inverse value of velocity of the sources are dependent on the large details of the distributions of sources. Finally, we note that by using these formulas it is possible to give the form of the expansions for the inverse value of the dimensionless Froude number $v_0/N\ell$, using some characteristic dimension of the source as ℓ.

BIBLIOGRAPHY

1. Dokuchayev, V. P., Dolina, I. S., IZV. AN SSSR: FIZ. OKEANA I ATMOSFERY (News of the USSR Academy of Sciences: Physics of the Atmosphere and Ocean), Vol 13, No 6, 655, 1977.

2. Gorodtsov, V. A., Teodorovich, E. V., Preprint of the Institute of Mechanical Problems, No 114, 1978.

5303
CSO: 8144 /0872

UDC 910.2(261.3)

INTERNATIONAL EXPEDITION IN THE BALTIC SEA ON THE SHIP 'GIDROMET'

Moscow OKEANOLOGIYA in Russian Vol 21, No 1, Jan-Feb 81 pp 187-190

[Article by A. A. Aksenov, A. I. Blazhchishin, K. Vypikh, V. K. Gudelis and B. Rosa]

[Text] In accordance with a plan of the Coordination Center of the Member Countries of the Soviet Economic Bloc Under the "World Ocean" Program, during the period 1-30 June 1979 specialists aboard the "Gidromet" (Polish People's Republic) carried out the first international expedition for study of Holocene shorelines and features on the floor of the Baltic Sea. Participating in the expedition were Polish specialists of the Institute of Meteorology and Water Management (Gdynia) and the Gdansk University and Soviet specialists from the Institute of Oceanology USSR Academy of Sciences, the Geography Division Academy of Sciences Lithuanian SSR and the Geology Institute Academy of Sciences Estonian SSR.

The work was carried out in the southeastern part of the Baltic Sea in two standard sectors of the Polish-Soviet economic zone (Fig. 1). A "Hantec" seismoprofilograph (Canada) was used in detecting the evidences of ancient shore levels and clarifying the structural details of the Quaternary stratum. This apparatus operated in a "boomer" regime. This apparatus makes it possible to register the fine structure of the Quaternary stratum with a high resolution (0.5-1 m). Using the "Hantec" profilograph it was also possible then to select the sites for the taking of cores of deposits -- at the sites of the surmised localization of ancient shore features. The cores were obtained using a modernized oscillating piston corer of the Kudinov design; the length of the cores was as great as 4.5 m. During the course of the expedition a total of 725 miles of seismic profiling work was done on 34 runs and 22 cores were obtained.

These investigations yielded new data on Holocene shore levels and the structure of the Quaternary stratum in the southeastern Baltic. As became clear from a preliminary analysis of the seismic profiles and data from vibrational drilling carried out earlier, in the Quaternary stratum, in the section south of the Slupskiy trench, there is a predominance not of moraines, but fluvioglacial sands, in the upper part reworked by the sea. The thickness of such sands on the land attains 100 m. In this respect Slupskaya Bank differs sharply from other shallow-water sectors of the Baltic Sea where the Holocene bottom profile was developed in the main moraine of the last glaciation. Two major antecedent valleys, oriented approximately parallel to the present-day shore, are situated between the coast of the Polish People's Republic and Slupskaya Bank. The valleys are incised in the fluvioglacial sands and were filled, according to data from vibrational drilling, by different continental formations, including peat bogs. The thickness of these

deposits attains 20-30 m; the thickness of the covering marine sands attains 3-4 m. Along the axis of the antecedent valleys there are several ancient lake basins filled with varved clays. On the eastern flank of Slupskaya Bank, under a layer of recent sands, it is possible to trace cut-off glaciodynamic structures which are the roots of pressure-created terminal moraine formations. Since the development of the shore zone in the Holocene occurred in the considered region against a background of an excess of sandy material, ancient shore levels are morphologically poorly expressed.

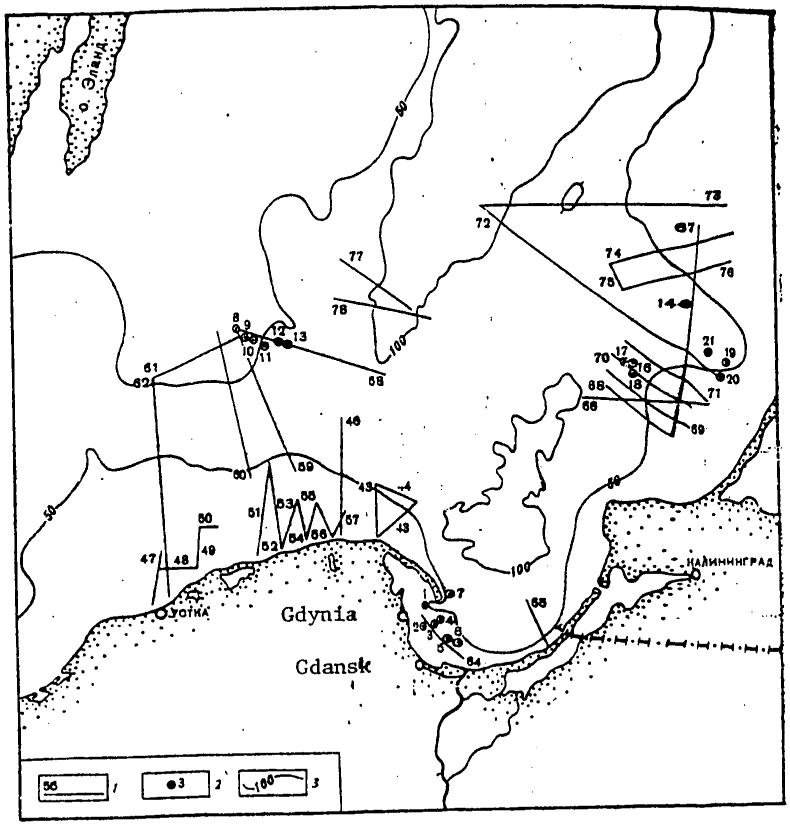

Fig. 1. Map of seismic profiling runs and position of stations. 1) seismic profiling runs; 2) position of vibrationally drilled holes; 3) isobaths, m

Ancient shore levels are traced more clearly on the southeastern slope of Yuzhnaya Srednyaya Bank. Here there are scarps at depths of 16, 20, 27, 32, 40, 61-62.5 m. The last of the scarps is evidently structural. A core of deposits with a length of about 3 m was obtained on the second scarp from above. Clearly represented in the core are shore formations exhibiting four major transgressive-regressive cycles and several lesser ones (Fig. 2). Each such cycle begins with a basal layer of gravelly-

pebbly sediment and ends with medium- and fine-grained sand. The great thickness of the basal layers of the major cycles suggests the superposing (intersecting) of several shorelines as a result of isostatic uplifting.

In the southwestern part of Gdansk Gulf there is an alluvial cone of the Vistula River which extends in a northwesterly direction to a depth of 30-40 m, dropping away in a steep scarp with a height of 30 m ("Kamerun"). According to data from seismic profiling, the cone consists of an obliquely layered stratum of sediments with a thickness of 20-30 m, lying in unconformity on Pleistocene clays, revealed by the cores in the deeper-water part of the gulf.

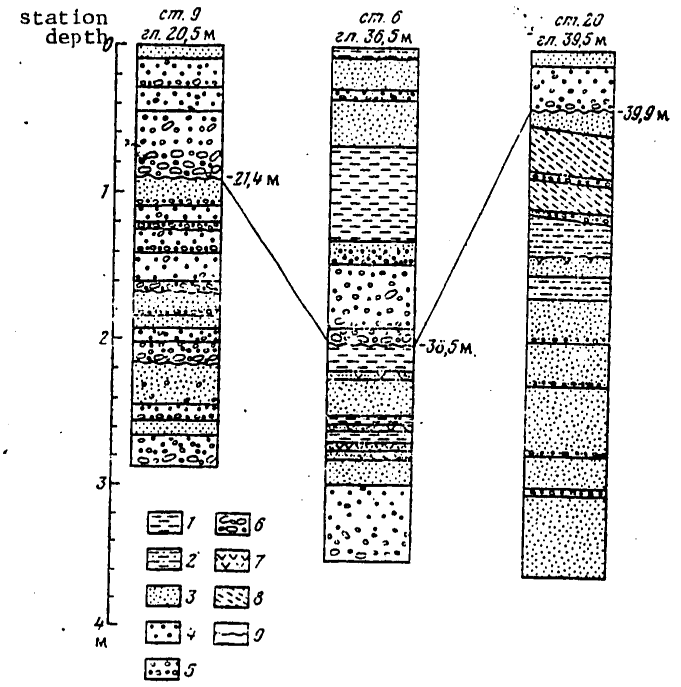

Fig. 2. Ancient shore formations in cores of Late Quaternary deposits (station 9 -- Yuzhnaya Srednyaya Bank, station 6 -- underwater cone of Vistula River, station 20 -- southern side of Neman antecedent valley). 1) aleuritic silt; 2) coarse silt; 3) medium- and fine-grained sand; 4) coarse-grained sand with gravel; 5) gravel; 6) pebbles; 7) peat; 8) obliquely layered sands; 9) transgressive boundaries.

As a result of vibrational drilling carried out at different bathymetric levels it was found that the obliquely layered stratum is represented by sands of different grain size and subordinate intercalations of gravels and silts. On the surface of

terraced areas -- silt depressions with depths of 30-34 m -- there are silts and aleuritic silts with a thickness up to 2 m or more, whereas in other sectors there are only sands. At readings from -30 to -40 m in the core sections it is possible to discriminate several peat intercalations, the thickest of which (40 cm) is at the levels -(31.7-32.1) m. In all probability, the time of formation of the peat deposits corresponds to the regression of Antsilovoye Lake. It was found that the reflecting boundaries on the seismograms are caused by basal horizons of gravel and pebbles forming as a result of the superposing of several transgressive-regressive cycles in the delta of the Vistula, growing during the course of the Holocene.

Two such major cycles are represented in the core taken at a depth of 36.5 m (Fig. 2, station 6). The lower cycle evidently corresponds to late boreal times and includes both basin and subaerial sediments. Ancient shore formations (pebbles and gravels), associated with the first littorine (?) transgression, are represented at the base of the upper cycle. An intercalation of silts in the middle part of the cycle possibly corresponds to the maximum level of the Littorine Sea.

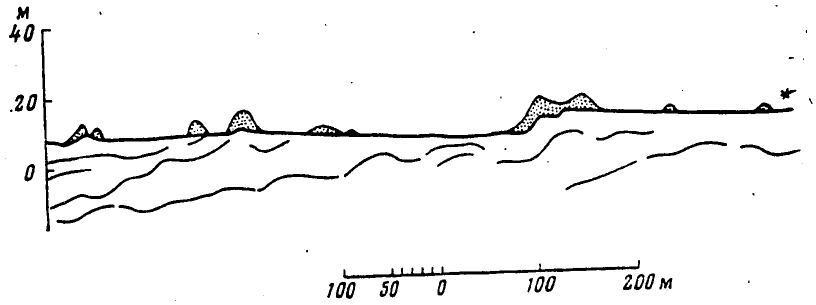

Fig. 3. Remnants of ancient eolian accumulations on the northern slope of the Kurshskoye Plateau (copied from seismogram, profile 72). For the location of the profile see Fig. 1.

In the northeastern part of Gdansk Basin and in the adjacent shallow waters a study was made of slope discontinuities and planation surfaces. The most interesting data were obtained on profile 72 (Kurshskaya Kosa - Gotland Depression) (see Fig. 1). Here a number of scarps and profile discontinuities can be detected. In a number of cases the good quality of the seismograms makes possible an unambiguous identification of these levels either as ancient shore formations or as structural or lithological. For example, a scarp of 66-72 m on the western slope of the Liyepaya Rise is caused by Devonian clint, whereas the eastern boundary of the Gdansk depression is expressed by a gentle but distinct discontinuity of the bottom profile (64-72 m), whose formation was evidently caused by incising of a glacial tongue into the edge of the Polish-Lithuanian syneclise. The ancient shore scarps and the abrasional terraced surfaces, traced at depths from 66 to 63 m, are possibly Lower Holocene (Yoldian), since in the paleontologically studied cores from this region preboreal layers are discovered at depths below 55 m. With respect to the lower levels (62-66, 64-68,

71-74 m), they cannot be regarded as Holocene shorelines. The highest of the traced levels have absolute readings from -(32-35) to -(35-39) m and evidently correspond to the shoreline of Antsilovoye Lake.

Interesting formations associated with the shoreline of this basin have been discovered in the northeastern part of the Kurshskoye morainal plateau. These accumulative bodies (horizontally measuring from 15 to 100 m and in height 1-2 m) were precipitated onto the structural (cuesta) scarps of the Upper Cretaceous substrate covered with a thin layering of coarse fragmented sediments remaining from erosion of the moraine (Fig. 3). In all probability these bodies represent the remnants of ancient dunes.

A core with a length of 3.6 m (see Fig. 2, station 20) was obtained from the southern edge of the Neman antecedent valley. It contains accumulative formations associated with the incising of this valley and its subsequent filling with Holocene sediments. The upper basal horizon of coarse and fine gravel in this core can be compared with the ancient shore formations of the first phase of the littorine transgression. The obliquely layered beds of sands and silts, which lie underneath in places, evidently represent a delta facies. The sediments of this facies along the uneven (but not basal) boundary lie on fine-grained sands and silts of marine or eolian genesis. It is difficult to identify the lower-lying layers.

On the basis of a preliminary analysis of the materials obtained on the expedition it is clear that the position of the ancient shore levels detected in the southeastern part of the Baltic does not fully correspond to that predicted theoretically as a result of isostatic adjustments. In the region of the Sambiyskiy Peninsula and Kurshskaya Kosa, on the one hand, and in the region of the southern part of Gdansk Gulf, on the other hand, the position of the Holocene levels is virtually identical. As can be seen from Fig. 2, the transgressive boundary between the littorine and Antsilovskiye sediments in the cores from these regions is at the levels -(38.5-39.9) m. At the same time, on the southern slope of Yuzhnaya Srednyaya Bank (station 9) this level is at the reading -21.4 m, that is, the relative value of the isostatic rise between the mentioned readings is approximately 17-18 m.

Investigations by the member countries of the Socialist Economic Bloc on the problem of Holocene ancient shorelines and coastal formations in the Baltic Sea will be continued.

5303
CSO: 1865/93

UDC 910.2(261)

THIRTY-FIRST VOYAGE OF THE SCIENTIFIC RESEARCH SHIP 'AKADEMIK KURCHATOV' (PRINCIPAL SCIENTIFIC RESULTS)

Moscow OKEANOLOGIYA in Russian Vol 21, No 1, Jan-Feb 81 pp 183-187

[Article by V. G. Kort]

[Text] The principal objective of the expedition during the 31st voyage of the scientific research ship "Akademik Kurchatov" was a study of the mesoscale (synoptic) spatial-temporal variability of hydrophysical fields (currents, temperature, density) in the regions of the eastern part of the subtropical zone of the Atlantic Ocean. The investigations were planned as a development of the studies carried out under the Soviet-American POLIMODE program. In accordance with this program, during the period 1977-1978 Soviet scientists, working in the southwestern part of the North Atlantic, carried out investigations of the dynamics of ocean currents in a long-term (more than one year) hydrophysical polygon; during this same time American expeditions carried out investigations in the central part of the North Atlantic. As a result of investigations under the POLIMODE program (USSR, United States), Poligon-70 (USSR) and MODE (United States), it was possible to obtain unique data on the dynamics of mesoscale movements in the ocean and study the dynamics of synoptic eddies in the western half of the subtropical zone of the North Atlantic. It was established that the synoptic eddies, having a great kinetic energy, are propagated from the eastern half of the ocean.

The implementation of investigations in the eastern part of the North Atlantic should clarify the regions of generation of eddy systems of a synoptic scale and supplement our knowledge concerning the dynamics of ocean currents in this poorly studied region.

The general region of the investigations was bounded by the meridians 20 and 40°W and the latitudes 20 and 40°N. The expedition lasted 105 days. The track followed by the expedition is shown in Fig. 1. The expedition worked from 17 April to 31 July 1980. The expedition was headed by Corresponding Member USSR Academy of Sciences V. G. Kort. The scientific research ship "Akademik Kurchatov" was commanded by captain of distant navigation K. V. Sokolov.

The scientific program of the expedition included: investigations of evolution of eddies in the open ocean under the influence of the mean current, atmospheric processes and topogenic factors; study of the dynamic, energy and biohydrochemical

characteristics of eddy disturbances in the ocean; study of the geographical distribution of eddies in the ocean; investigation of the spatial-temporal variability of primary hydrooptical characteristics of the ocean in dependence on hydrological conditions and other factors; a complex of studies on heat exchange between the ocean and the atmosphere; aerological observations.

During the voyage three quasisynchronous hydrological surveys were made of regions of the passage of the anticyclonic eddy discovered at the beginning of the work; seven self-contained autonomous oceanographic buoy stations with automatic current recorders and automatic water temperature recorders operated in the field of the investigated eddy for a total of 30-35 days. Temperature sounding of the upper layer in the ocean (0-500 m) was carried out each 20-30 miles on 30 runs with a total extent of more than 20,000 km. Along the entire track of the vessel there was aerological sounding (once a day), meteorological and actinometric observations. About 9,000 hydrochemical determinations were made in water samples. Measurements were made at 85 hydrooptical stations. More than 200 biological samples were collected.

The primary processing of observational data and preliminary processing were carried out during the course of the voyage. The principal results of this analysis are given below for different aspects of the program.

1. Meteorology. With transition from spring to summer two periods can be discriminated in the formation of the Azores High: during the first period the weather map does not show the Azores High as a unified pressure formation and in most cases the pressure field has two or three centers. This period is assigned to spring. The second period, summer, is a time when the Azores High is well formed and constitutes a single-center pressure formation. In spring there are winds from all eight directions, whereas in summer -- only from the NE, E and SE, with a predominance of winds of a purely easterly direction. The center of the Azores High experiences a looping movement in a counterclockwise direction. On the northern periphery of the Azores High there is usually no air temperature inversion in the lower troposphere (1-3 km) due to the cyclonic activity in the temperate latitudes. In the southern half of the anticyclone, facing the equator, a temperature inversion is observed everywhere, both near the center of the anticyclone and on its periphery. Changing its thickness and intensity, the inversion exists daily.

The stratocumulus clouds beneath inversions have a very strong variability: in the course of 15-20 minutes the clouds can scatter or cover the entire sky. The albedo of the ocean surface was low -- ~5% and therefore a great part of the heat reaches the ocean surface and is absorbed by it. The mean daily values of total solar radiation are as follows: 578, 668, 512 cal.cm^{-2}.day^{-1} for periods I, II, III respectively. The interaction between the ocean and the atmosphere leads to the following values of the heat balance components for the ocean surface by periods:

		R	P	LE	E
I	9-16 May	477	2.2	85	0.145
II	6-21 Jun	555	8.6	154	0.264
III	5-15 Jul	422	8.6	144	0.247

where R is the radiation balance; P is turbulent heat exchange; LE is the expenditure of heat on evaporation (all three parameters are expressed in cal·cm^{-2}·day^{-1}); E is evaporation from the ocean, cm·day^{-1}.

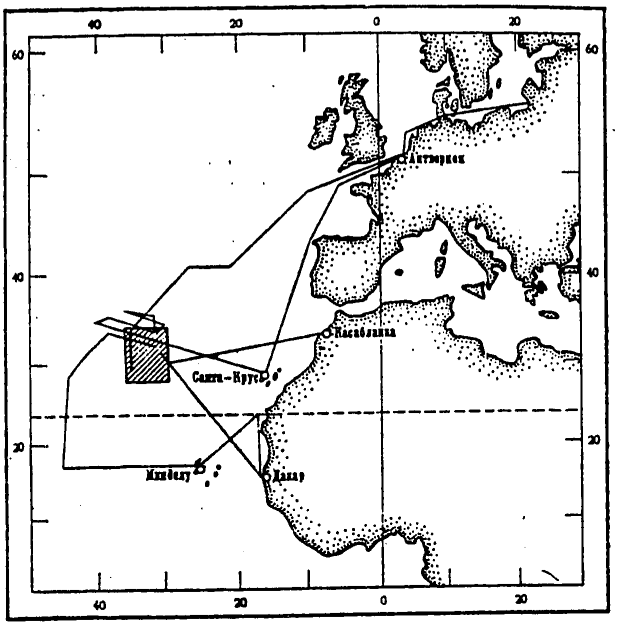

Fig. 1. Map of track and work on 31st voyage of scientific research vessel "Akademik Kurchatov." The solid lines represent temperature runs made with the T30-1. The shaded polygon represents the region of successive hydrological surveys of the anticyclonic eddy.

2. Hydrology. Three quasisynchronous hydrological surveys made it possible to trace the evolution of the mesoscale anticyclonic eddy discovered early in May to the southwest of the Azores (at a distance of 300 miles) (Fig. 2). In the first stage (11-15 May) the anticyclonic eddy had a mean diameter for the 15° isotherm of 250-300 km and a depth of displacement of this isotherm 75-100 m. The eddy was traced to the horizon 1,500 m. The central region of the eddy had the coordinates 32°30'N, 31°30'W.

The second hydrological survey (13-21 June) indicated some weakening of the eddy. Its mean diameter decreased to 200 km and the displacement of the 15° isotherm attained 50-60 m. The coordinates of the central region of the eddy were 30°30'N, 33°40'W. Thus, after approximately 30 days the eddy had moved 370 km in a southwesterly direction with a mean velocity 10-12 km·day^{-1}.

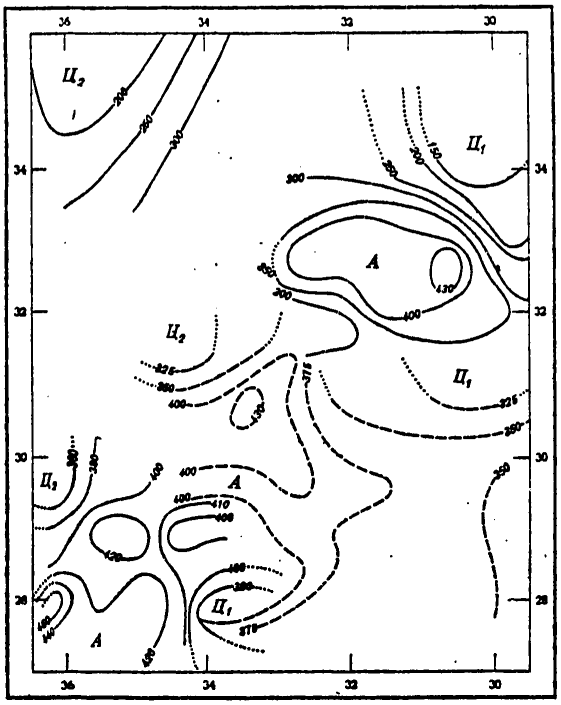

Fig. 2. Topography of isothermic surface 15°C according to data from hydrological surveys. The solid isolines represent depths of the 15°C isotherm in m according to data from the first and third surveys; the dashed isolines -- same for the second survey. $Ц_{1,2}$ -- cyclonic eddies; A -- anticyclonic eddy whose evolution was investigated.

At the time of the third survey (9-13 July) the core of the eddy had divided into three parts of different intensity and the eddy itself had essentially decayed. The entire region of individual eddy cores was pressed between two cyclonic eddies which had followed the anticyclone from the first stage of its investigation. The central region of the breaking-up anticyclone had the coordinates 28°00'N, 35°30'W. During the period between the second and third surveys the eddy moved a distance of 320 km to the southwest with a mean velocity 11 km·day^{-1} or 13 cm·sec^{-1}. The identity of the anticyclonic eddy in all three stages of the survey is confirmed both by the general character of the eddy field in the polygons of the hydrological surveys and by the distribution of the hydrological and hydrochemical characteristics in the eddy region.

Prior to completion of the total processing of the observational data and their analysis it is difficult to determine the nature of the investigated anticyclonic eddy. However, the distribution and structure of the hydrological and hydrochemical characteristics quite definitely indicate the capture and transport of different water masses by this eddy. It can be assumed that the investigated eddy is

a mesoscale topographic eddy. The complex and sharply changing bottom relief and the hydrological regime in the region of eddy propagation to a certain degree confirm this hypothesis.

Instrumental measurements of currents with three autonomous buoy stations during the first period of the investigations indicated the existence of rather strong ebb-and-flow and inertial currents in the region.

The orbital velocities in the investigated anticyclonic eddy on the average attained: at the horizon 200 m -- 20 $cm \cdot sec^{-1}$, at 400 m -- 23-25, at 700-800 m -- 15-20 and at 1,500 m -- 6-8 $cm \cdot sec^{-1}$.

The geographical distribution of mesoscale eddies in the eastern part of the North Atlantic was investigated on 15 transoceanic temperature runs (in the layer 0-500 m) with a total length of 16,500 km. A total of 26 clearly expressed cyclonic and anticyclonic mesoscale eddies were registered. These had a mean diameter of 200-250 km and a mean movement of the 15° isotherm of 100-150 m. Most of the discovered eddies were concentrated around the Azores region, especially to the southwest of these islands. The ocean region bounded by the western shore of Africa on the east, the Mid-Atlantic Ridge on the west and 16-28°N, was poorest in mesoscale eddies. In most cases the discovered mesoscale eddies correlate with sharp rises of the ocean floor. This correlation is closest in the regions of passage of the Canaries, North Trades and North Atlantic Currents over sea rises and ridges. It can be asserted that the Azores Islands region is the site of the most intensive generation of mesoscale eddies in the eastern Atlantic.

Hydrochemistry. A very detailed study was made of the chemical structure and evolution of the anticyclonic eddy in time and space on the basis of five quasiconservative chemical indices -- dissolved oxygen, silicon, phosphorus, pH and alkalinity to depths of 1,700-2,000 m.

Maps of the distribution of dissolved oxygen and silicon made it possible to judge the evolution of the anticyclonic eddy in time and space, especially at moderate and great depths. The combination of the five chemical parameters and salinity give basis for asserting that one and the same anticyclonic eddy was investigated in the three surveys.

The entire investigated region is characterized by an oxygen supersaturation of the entire surface layer with a thickness of 70-140 m on the average by 4% (per 0.2 ml). With respect to CO_2 the picture is the opposite -- at the ocean surface the CO_2 content is less than in the near-water layer of the atmosphere and the ocean absorbs CO_2 from it proportional to the wind velocity and the difference in the partial pressures of CO_2 in the water and atmosphere.

Much material was collected on the content of organic carbon in the water (more than 200 determinations). It was experimentally established that the results of the determinations of C_{org} with the S. V. Lyutsarev instrument must be modified by a correction of 1 mg C/liter, which is not less than 30-50% of the measured values.

4. Hydrooptics. More than 80 hydrooptical stations were occupied during the voyage. These investigations revealed the high purity and spatial homogeneity of the waters in the investigated region. This applies, in particular, to the spectral absorption values, which are close to the values adopted for pure distilled water. The spectral attenuation values in the surface layer experience appreciable fluctuations, but for the most part they are in the limits characteristic for very pure surface waters.

A great volume of information was collected on the variability of the vertical profiles of small-angle scattering (about 400 vertical profiles were measured) and investigations were also carried out in processing the results of remote methods for determining the optical properties of sea water, the content of chlorophyll and suspensions in the surface layer of the ocean.

Data from measurements made using a spectral instrument for determining irradiance from above, sea and sky brightness, installed at the ship's prow, agree well with data from direct measurements of optical properties; the chlorophyll concentrations computed on the basis of these data fall in the range 0.06-0.10 $mg \cdot m^{-3}$, characteristic for biologically very impoverished regions of the ocean.

5. Hydrobiology. In the course of the voyage there were 31 successful trawlings with the trawl at different depths from 75 to 700 m and as a result of the first sorting of material there were 248 samples of different groups of macroplankton organisms. All the samples were weighed for subsequent computations of biomass. All the fish were determined; it was established that the collection included 117 species.

Phytoplankton collections were made at 106 stations. Thirty-five full bathometric series were run in the layer 100-0 m and 202 catches were taken with a large net in this same layer; the total number of samples was 590. During the voyage 130 bathometric samples and 10 net samples were processed; 188 forms of phytoplankton were determined down to the species level.

The region to the northeast of the Cape Verde Islands was the richest with respect to the biomass of mesopelagic fish (15 $g/10^4$ m^3); this was followed by the regions to the south of the Azores Islands (10 $g/10^4$ m^3) and the central part of the ocean (6 $g/10^4$ m^{-3}). The poorest region was that between the Madeira Islands and the coast of Morocco (< 5 $g/10^4$ m^3), which contradicts the general opinion that there is a high biological productivity of these waters and this merits special analysis.

We should note the presence of several equatorial species of mesopelagic fish in the zone of the Canaries Current, near the Cape Verde Islands. This is apparently evidence of the penetration here of waters of equatorial origin. In this same region there was found to be a species of fluorescent anchovies which is new for the region.

The phytoplankton of the investigated regions was extremely impoverished (less than 1,000 cells per liter), but the region to the east of the Madeira Islands (less than 300 cells per liter) stands out as being especially impoverished, as it is with respect to the biomass of abyssal fish. The general impoverishment of plankton flora is attributable both to the fact that a great part of the work was carried

out in oligotrophic waters and to the fact that this coincided in time with the period of the summer minimum of the population of phytoplankton and biogenous elements.

The finding of several arctic-boreal forms to the south of the Azores Islands gives basis for regarding this region as the southern part of the zone of mixing of tropical and arctic-boreal plankton flora.

It was established as a result of use of a new method for the processing of phytoplankton samples (the so-called reverse filtering method) that the population of plankton algae in the oligotrophic waters of the Northeast Atlantic is an order of magnitude greater than was assumed earlier.

5303
CSO: 1865/93

UDC 551.466.81

LINEAR MECHANISM OF FORMATION OF THE SPECTRUM OF INTERNAL WAVES IN THE OCEAN

Moscow IZVESTIYA AKADEMII NAUK SSSR: FIZIKA ATMOSFERY I OKEANA in Russian Vol 16, No 9, Sep 80 pp 992-996

[Article by V. A. Sokolov, L. M. Fomin and A. D. Yampol'skiy, Institute of Oceanology USSR Academy of Sciences, manuscript submitted 12 Dec 78, resubmitted after revision 22 Aug 79]

[Text] As indicated by measurements, movements of the internal waves type are always present in the ocean [1]; they can have greater or lesser energy and have a different distribution of amplitudes of oscillation in the vertical profile, which is probably associated with local conditions of stratification and the intensity and spectral structure of the external effect, exciting internal waves. [2]. High-frequency internal waves are observed most clearly in the thermocline region, where the vertical density gradient is not small. Another peculiarity of internal waves is their temporal intermittence: usually the record of fluctuation of water temperature or the vertical velocity component at a point resembles the record of a signal with amplitude modulation; the predominant value of the carrier frequency of the fluctuations will be less than the local value of the Väisälä frequency [3].

On the basis of general considerations the mechanism of the formation of internal waves can be represented in the following way. If some force (fluctuations of atmospheric pressure or wind velocity) acts on the water layer or at the ocean surface, leading to vertical displacements of water particles in the thermocline region, in addition to the forced oscillations there should be free oscillations at the local Väisälä frequency. The latter will have the greater energy the greater the set of spatial scales of the external effect which will cover the range of wave number values satisfying the dispersion relationship for internal waves.

In the real ocean the Väisälä frequency changes with depth; there should be a combining of the fluctuations at closely spaced levels due to the continuity of movement of the water. In the simplest case this is similar to the addition of sinusoidal signals at close frequencies and the appearance of an amplitude-modulated oscillation with a carrier frequency $(\omega_1 + \omega_2)/2$. In the case of a continuous stratification of water the mechanism of linear interaction of fluctuations at different horizons will be more complex, leading to the formation of a whole spectrum of internal waves with the properties noted above.

Thus, we will examine how the spectrum of internal waves changes with depth in dependence on stratification conditions with an identical external effect. Such a formulation is in some sense a special case of a more general formulation of the problem by A. I. Leonov and Yu. Z. Miropol'skiy [2], who investigated the mechanism of generation of internal waves in dependence on the type of external effect spectrum.

In our examination of the vertical and temporal structure of high-frequency internal waves in a layer of a nonrotating stratified fluid we will write the following system of equations:

$$\frac{\partial w}{\partial t} - \frac{g}{\rho_0}\rho + \frac{1}{\rho_0}\frac{\partial P}{\partial z} = 0, \quad \frac{\partial u}{\partial t} + \frac{1}{\rho_0}\frac{\partial P}{\partial x} = 0,$$

$$\frac{\partial \rho}{\partial t} + w\frac{\partial \rho_0}{\partial z} = 0, \quad \frac{\partial u}{\partial x} + \frac{\partial w}{\partial z} = 0, \tag{1}$$

where u, w are the horizontal and vertical velocity components; P is pressure; $\rho = \rho(x, z, t)$; $\rho_0 = \rho_0(z)$ is water density; g is the acceleration of gravity; the z-axis is directed downward; the x-axis is directed horizontally. It is postulated that the sought-for functions are not dependent on the second horizontal coordinate.

The system of equations (1) is easily reduced to one equation for the stream function

$$\frac{\partial^2}{\partial t^2}\nabla^2\psi + N^2(z)\frac{\partial^2\psi}{\partial x^2} = 0,$$

$$\nabla^2 = \frac{\partial^2}{\partial x^2} + \frac{\partial^2}{\partial z^2}. \tag{2}$$

Here $\partial\psi/\partial x = -w$, $\partial\psi/\partial z = u$, $N^2(z) = gd\ \ln\rho_0/dz$ is the Väisälä frequency.

We will also use the boundary conditions: $\psi = 0$ at the initial moment in time (with $t = 0$) and at the bottom (with $z = H$); at the free surface of the ocean with $z = 0$

$$\psi = \sum_n A_n \sin(k_n x - \omega_n t) \quad \text{with } 0 \leqslant t \leqslant T_0,$$

$$\psi = 0 \quad \text{with } t > T_0, \tag{3}$$

the periodicity conditions $\psi_{x=0} = \psi_{x=L}$ are used at the lateral boundaries of the region.

The boundary condition (3) simulates some external effect disturbing the stably stratified initially at-rest fluid. The physical nature of this effect can be any which is desired (this is unimportant for us); this can be the effect of the field of atmospheric pressure. The absolute value of this external effect also does not have a high value because within the framework of linear problems the nature of the solution cannot change. For the sake of clarity it can be assumed that with stipulated horizontal and vertical scales the external effect is characterized by a vertical velocity of about 0.01 $cm \cdot sec^{-1}$. In the numerical computations discussed below the frequency ω_n was selected equal to the value of the

Väisälä frequency at the ocean surface in order to free the results of the computations in the water thickness from a forced wave propagating upward to the jump layer. The time of operation of the "external effect" T_0 was selected small in comparison with the period of the Väisälä oscillation at the ocean surface but was adequate for the entrainment into movement of a considerable thickness of water and for all practical purposes was $T_0N(0)/2\pi < 0.5$. As a result of such a restriction imposed on the boundary condition, during almost the entire time of the numerical computations with a set of records of internal waves at different horizons there was satisfaction of the "solid cap" condition at the ocean surface and the solution corresponded to the free oscillations in the water layer -- the reaction of the ocean to a short-term external effect. Internal waves generated by the random pressure field were examined in [2].

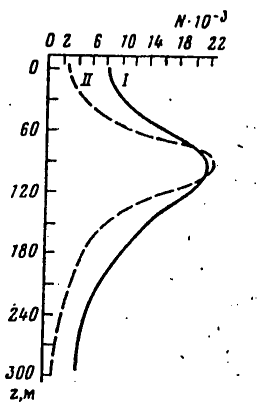

Fig. 1. Vertical distribution of Väisälä-Brent frequency.

A zero boundary condition with z = 0 was introduced into the solution at the time T_0, when all the considered layer of fluid was entrained into oscillatory movement; T_0 usually did not exceed 30 minutes.

For convenience in numerical solution the equation (2) was replaced by the system of equations

$$\frac{\partial^2\xi}{\partial t^2} + N^2(z)\frac{\partial^2\psi}{\partial x^2} = 0, \quad \nabla^2\psi = \xi. \tag{4}$$

The unknown functions were expanded into a Fourier series relative to the variable x; the derived system of equations for the set of wave numbers k_{xj} was solved numerically with a finite-difference approximation with a second order of accuracy relative to the variables z and t. The resulting solutions were reduced to the space (x, z, t) by an inverse Fourier transform. The rapid Fourier transform was used for direct and inverse transforms.

The region for the solution is a rectangle in the space (x, z), $0 \leqslant x_j < L$, $0 \leqslant z_i \leqslant z$, L = 1280 m, z = 320 m, Δx = 40 m, Δz = 10 m.

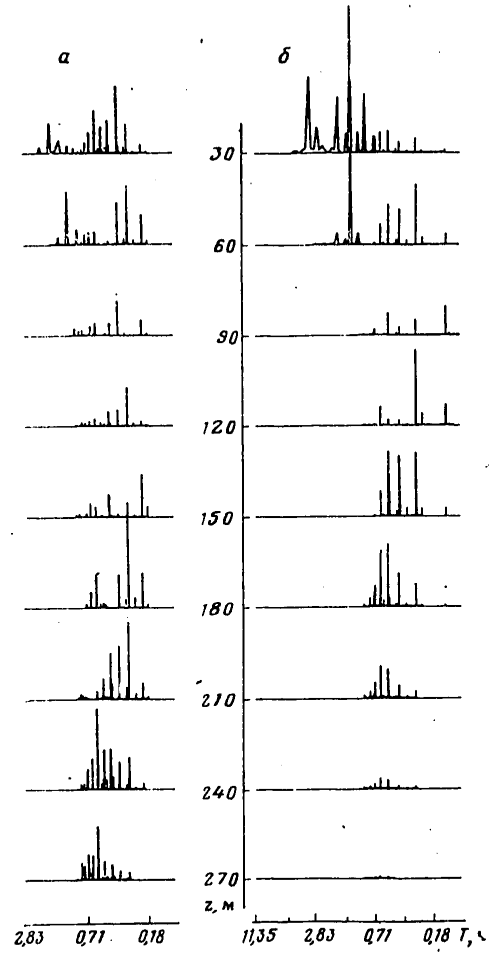

Fig. 2. Spectra of vertical component of velocity at different horizons: a) profile of Väisälä frequency I; b) profile of Väisälä frequency II. $k_1 = 2\pi/L_1$, $k_2 = 2\pi/L_2$; L_1 = 250 m, L_2 = 425 m; $A_1 = A_2 = 0.5$.

The solution was obtained with the interval Δt = 20 sec in the course of 45.7 hours model time, which ensured a set of series of the values of the sought-for functions adequate in length for their spectral representation.

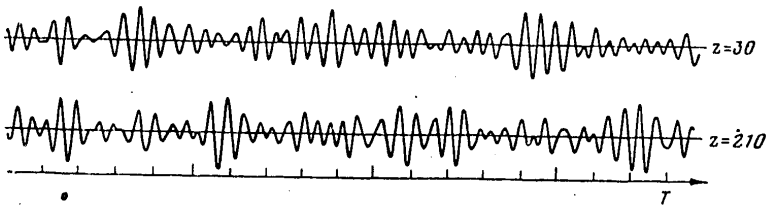

Fig. 3. Curves of the temporal variability of the vertical velocity component at different horizons.

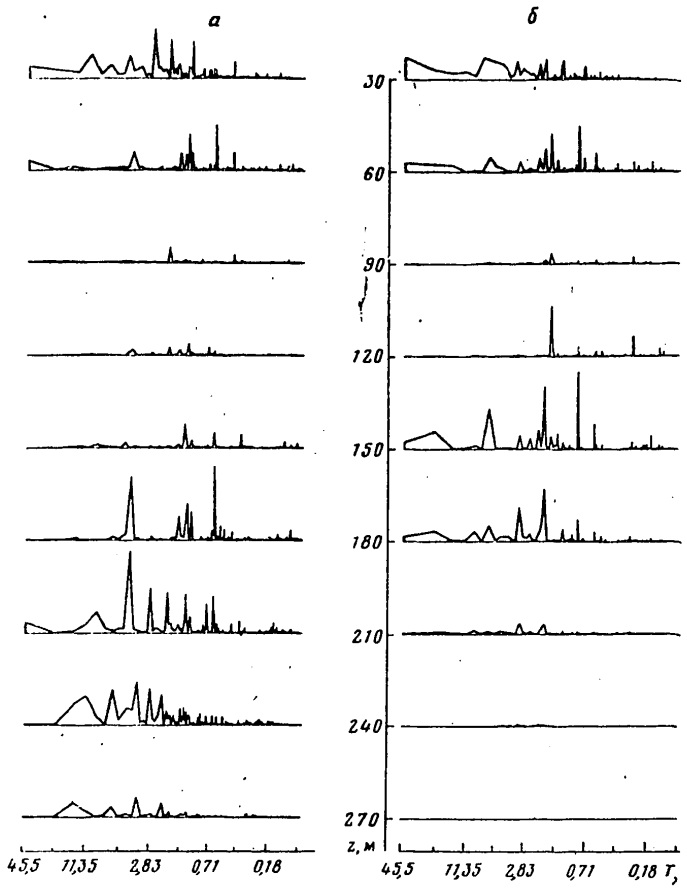

Fig. 4. Spectra of square of vertical velocity component at different horizons: a) for profile of Väisälä frequency I; b) for profile of Väisälä frequency II.

Several variants of the problem were calculated for two vertical profiles of the Väisälä frequency, shown in Fig. 1. One of them has a more clearly expressed water density jump layer and a great range of the values of the Väisälä frequency in comparison with the second profile.

As the horizontal scale of the external effect entering into the boundary condition (3) we took a set of values of the wave numbers corresponding to wave lengths from several tens to hundreds of meters. With a wave length of 100 m or less internal waves do not penetrate under the density jump layer and the nonzero values of the solution are concentrated in the upper layer of the ocean; the deep layers remain at rest. With wave lengths of 250 and 425 m (a greater length was not used in the computations) internal waves are generated in the entire water layer from the surface to the bottom.

Figure 2 shows the energy spectra of the vertical velocity component for internal waves at several horizons in the case of two-wave stipulation of the boundary condition (3), $A_1 = A_2 = 0.5$. Their line structure is associated with discrete stipulation of the vertical profile of the Väisälä frequency. With a decrease in the vertical interval the number of peaks in the spectrum will increase and the spectrum of the vertical velocity component will tend to become continuous, but possibly with several maxima.

Figure 2 shows also that fluctuations in the entire layer occur at frequencies less than the local buoyancy frequency; this frequency difference is maximum in the density jump layer and decreases above and below it. Only in the deep layers, where the vertical gradient of the Väisälä gradient is small, can the fluctuations occur at frequencies close to the local Väisälä frequency.

The energy of fluctuation of the vertical velocity component in internal waves has a minimum in the density jump layer and increases beyond its limits. It becomes equal to zero at the ocean surface and at the bottom (by virtue of the boundary conditions). When there is a sharply expressed density jump layer (Fig. 2,b) it can be seen that there is attenuation of the energy of fluctuations with depth: in the bottom layer deeper than 270 m the amplitude of the fluctuations is very small. With a smoother vertical distribution of the Väisälä frequency the intermediate maximum of the energy of fluctuations is shifted in the direction of the bottom and the waves penetrate to a greater depth (Fig. 2,a).

On the records of the vertical velocity component the existence of a peaklike spectrum w is manifested in that the w(t) curves have the appearance of oscillations with amplitude modulation (Fig. 3).

It makes sense to examine the form of the spectrum of the square of the vertical velocity component in internal waves since the square of vertical velocity with averaging forms one of the components of Reynolds stress, which can be important for lower-frequency spectral components of movement in the ocean, for example, for inertial fluctuations. The appearance of the w^2 energy spectrum is shown in Fig. 4. The energy of the square of the vertical velocity component is distributed in a broader frequency range extending to the left and to the right of the local Väisälä frequency value. It has a minimum in the density jump layer and maxima at the intermediate horizons. Behavior of the w^2 spectrum in the LF region is of interest since with averaging for computation of the Reynolds stress the high-frequency part of the w^2 spectrum drops out. [For computing the Reynolds stress it is necessary to average w^2 in a time equal to several values of the predominant period of the internal waves. In our case averaging for 5-10 hours is adequate.]

Figure 4 shows that internal waves generate Reynolds stresses in two layers associated with the upper and lower boundaries of the density jump layer. For the first vertical profile of the Väisälä frequency these layers are situated at depths of about 30 and 210 m; for the second -- about 30 and 150-180 m. In the vertical profile of the Väisälä frequency the mentioned depths correspond to the depths of the maxima of its curvature.

As follows from the form of the w^2 spectrum, the Reynolds stresses generated by the high-frequency internal waves (we will call them Väisälä waves) contain harmonic components with frequencies overlapping the range of frequency values for the inertial fluctuations. This circumstance can be very important for understanding the mechanism of appearance of inertial fluctuations of velocity in the ocean since a periodic force (Reynolds stress) with the period of inertial fluctuations appears in the equations describing inertial movement.

In obtaining a numerical solution of the simple linear problem of formation of the spectrum of Väisälä internal waves in the ocean we obtained a result agreeing satisfactorily with the experimental data. It follows from the solution that:

1) the depth of penetration of the Väisälä waves is dependent on the peculiarities of the vertical distribution of water density and the structure of the external effect;
2) the energy of the internal waves is distributed in some frequency range whose values are less than the local Väisälä frequency at a particular horizon;
3) the energy of the Väisälä waves is maximum at the upper and lower boundaries of the water density jump layer;
4) Väisälä waves generate Reynolds stresses whose energy spectrum overlaps the range of frequency values for inertial fluctuations.

These conclusions do not contradict the experimental data.

BIBLIOGRAPHY

1. Sabinin, K. D., "Some Characteristics of Short-Period Internal Waves in the Ocean," IZV. AN SSSR, FAO (News of the USSR Academy of Sciences, Physics of the Atmosphere and Ocean), 9, No 1, 1973.

2. Leonov, A. I., Miropol'skiy, Yu. Z., "Generation of Internal Waves in the Ocean," MEZHDUNARODNYY SIMPOZIUM PO STRATIFITSIROVANNYM TECHENIYAM (International Symposium on Stratified Currents), Novosibirsk, 1972.

3. Miropol'skiy, Yu. Z., Monin, A. S., "Internal Waves," OKEANOLOGIYA, FIZIKA OKEANA (Oceanology, Physics of the Ocean), Vol 2, Moscow, "Nauka," 1978.

5303
CSO: 1865/63

UDC 551.466.81

GENERATION OF INTERNAL WAVES DURING THE UNIFORM LINEAR MOTION OF LOCAL AND NONLOCAL SOURCES

Moscow IZVESTIYA AKADEMII NAUK SSSR: FIZIKA ATMOSFERY I OKEANA in Russian Vol 16, No 9, Sep 80 pp 954-961

[Article by V. A. Gorodtsov and E. V. Teodorovich, Institute of Mechanical Problems USSR Academy of Sciences, manuscript submitted 21 Jun 79, resubmitted after revision 2 Oct 79]

[Text]

Abstract: It is shown that a shortcoming of the problem of generation of internal waves by a moving point source (and a combination of point sources in the form of a dipole) in the case of an exponential stratification of fluid is an infinity of such values as the total generation energy and the pressure field on the axes at the source. Divergence disappears when allowance is made for the nonlocality of the sources. Precise solutions are analyzed for nonlocalities of the spherically symmetric, plane and linear types.

In a number of studies [1-11] computations of the field of linear internal waves generated during the movement of bodies in a density-stratified fluid were carried out on the basis of modeling of the bodies by systems of point sources. The problem has been analyzed using approximate asymptotic methods and many features and shortcomings of such modeling were given no attention. In our study we obtained some precise results for the simplest case of an unbounded exponentially stratified fluid. In particular, the problem of the total energy of generation of internal waves is considered.

1. Hydrodynamic Fields of Moving Nonlocal Sources

Small perturbations of velocity v, pressure p and density ρ in an exponentially stratified incompressible fluid in the presence of a source of the mass m(r,t) are described by the system of equations [12]

$$\frac{\partial \mathbf{v}}{\partial t}+\nabla p=\rho \mathbf{g},\quad \frac{\partial \rho}{\partial t}+\frac{N^2}{g}\mathbf{g}\mathbf{v}=0,\quad \nabla \mathbf{v}=m.$$

As a simplification here use was made of the Boussinesq approximation and after introduction of the Väisälä-Brent constant frequency N the density of the unperturbed state is assumed equal to unity.

From this system of equations it is possible to derive another equation for the scalar potential $\psi(r, t)$ through whose derivatives all the sought-for parameters are expressed (the movements are considered eddy-free in the horizontal plane)

$$\mathcal{L}\psi=-m, \quad \mathcal{L}\equiv\frac{\partial^2}{\partial t^2}\nabla^2+N^2\nabla_h^2, \quad p=\left(\frac{\partial^2}{\partial t^2}+N^2\right)\frac{\partial\psi}{\partial t},$$
$$\rho=\frac{N^2}{g}\frac{\partial^2\psi}{\partial z\partial t}, \quad v=-\left(\frac{\partial^2}{\partial t^2}\nabla+N^2\nabla_h\right)\psi. \tag{1}$$

Here $$\nabla=(\partial/\partial x, \partial/\partial y, \partial/\partial z), \quad \nabla_h=(\partial/\partial x, \partial/\partial y, 0),$$

and z is the vertical coordinate.

The solution of the equation for potential can be written using Green's "lagging" function in the form of the integral

$$\psi(\mathbf{r}, t)=-\int d^3r'dt'G^r(\mathbf{r}-\mathbf{r}', t-t')m(\mathbf{r}', t'), \tag{2}$$

where by the function $G^r(r, t)$ is meant solution of the equations

$$\mathcal{L}G^r(\mathbf{r}, t)=\delta(\mathbf{r})\delta(t), \quad G^r(\mathbf{r}, t)|_{t<0}=0, \tag{3}$$

and the last condition ensures a causal character of the time dependence in (2).

For a uniformly and linearly moving source of constant intensity $m(r,t) = m_0f(r - vt)$ the formula for potential can be rewritten in the form

$$\psi=-m_0\int d^3r'dt'G^r(\mathbf{r}_1-\mathbf{r}'+\mathbf{v}t', t')f(\mathbf{r}'), \quad \mathbf{r}_1=\mathbf{r}-\mathbf{v}t, \tag{4}$$

so that the stationarity of the field of perturbations in the coordinate system related to a moving source is obvious.

Other convenient integral representations are obtained when using Fourier expansions

$$G^r(\mathbf{r}, t)=\frac{1}{(2\pi)^4}\int d^3k\,d\omega G^r(\mathbf{k}, \omega)e^{i\mathbf{kr}-i\omega t}=$$
$$=\frac{1}{(2\pi)^2}\int dk_x\,d\omega G^r(k_x, y, z, \omega)e^{ik_xx-i\omega t}.$$

Here and in the text which follows for the Fourier components we will use the same symbols as for the initial parameters and they differ only with respect to the arguments.

Using these expansions the formula for the potential of a uniformly moving source can be transformed to the form

$$\psi=-\frac{m_0}{(2\pi)^3}\int d^3k\,d\omega G^r(\mathbf{k}, \omega)f(\mathbf{k})\delta(\omega-\mathbf{kv})e^{i\mathbf{kr}_1}, \tag{5}$$

$$\psi=-\frac{m_0}{2\pi}\int dk_x\,d\omega\,dr_\perp'G^r(k_x, \mathbf{r}_\perp-\mathbf{r}_\perp', \omega)f(k_x, \mathbf{r}_\perp')\delta(\omega-k_xv)e^{ik_xx_1}. \tag{6}$$

In the second representation we selected a special coordinate system in which the x-axis coincides with the direction of movement and $r_\perp$ is a two-dimensional transverse vector. Then we will limit ourselves to the case of a horizontally moving source and then the x-axis will be horizontal to the axis of movement. The appearance of the δ-function in these representations, indicating a linear relationship between frequency and the wave vector component in the direction of movement $\omega = kv$, is due to the stationary character of movement of the source (the dependence on the difference r - vt in the initial parameters).

For determining the form of the function $G^r(k_x, r_\perp, \omega)$ entering into the representation (6) we will use a Fourier expansion in the variables x, t. Then from (3) we obtain the equation

$$\left[(\omega^2-N^2)\frac{\partial^2}{\partial y^2}+\omega^2\frac{\partial^2}{\partial z^2}-(\omega^2-N^2)k_x^2\right]G^r(k_x, y, z, \omega)=-\delta(y)\delta(z),$$

in which the differential operator with $\omega^2 > N^2$ by a simple replacement of the variables is reduced to $\partial^2/\partial y'^2 + \partial^2/\partial z'^2 - \varkappa^2$.

The Green's function of such an operator is proportional to the cylindrical function $K_0(\varkappa\sqrt{y'^2 + z'^2})$ (for example, see [13]) and in the initial variables we have

$$G^r(k_x, y, z, \omega)|_{\omega^2>N^2}=\frac{K_0(|k_x\sqrt{q}/\omega|)}{2\pi|\omega|(\omega^2-N^2)^{1/4}} \qquad (7)$$
$$q=(\omega^2-N^2)z^2+\omega^2y^2.$$

By virtue of the causal character of Green's "lagging" function its Fourier components should be analytical functions of frequency in the upper half-plane of complex frequencies and therefore $G^r(k_x, y, z, \omega)$ with $\omega^2 < N^2$ can be determined by means of analytical continuation of expression (7) through the upper half-plane [12]. For positive frequencies $\omega < N$ for $G^r(k_x, y, z, \omega)$ we thus find the formula

$$G^r(k_x, y, z, \omega)|_{0<\omega<N}=$$
$$=-\frac{\theta(-q)}{4\omega\sqrt{N^2-\omega^2}}H_0^{(2)}(|k_x\sqrt{-q}/\omega|)-i\frac{\theta(q)}{2\pi\omega\sqrt{N^2-\omega^2}}K_0(|k_x\sqrt{q}/\omega|), \qquad (8)$$

and the expression with negative frequencies is obtained from it if we take into account the properties of Green's function and cylindrical functions (the line at top is the symbol for complex conjugation)

$$G^r(k_x, r_\perp, -\omega)=\overline{G^r(k_x, r_\perp, \omega)}, \quad \overline{H_0^{(2)}(\bar{x})}=H_0^{(1)}(x)=J_0(x)+iN_0(x). \qquad (9)$$

Without writing the rather unwieldy general formula for potential with this function $G^r(k_x, r_\perp, \omega)$ we will dwell on some special cases in which the formulas become simpler due to the special form of the nonlocal sources and the choice of the discriminated observation directions.

For a plane source in the form $f(r) = \delta(z)f_1(x,y) = \delta(z)f_1(-x,y)$ the potential difference in the plane of the source is described by the formula

$$\frac{\partial\psi}{\partial t}\Big|_{z=0}=\frac{m_0}{2\pi^2 v}\int dy'\left\{\int_0^{\pi/2}d\alpha K_0(\xi\cos\alpha)f_1\left(\frac{N}{v}\cos\alpha,y'\right)\cos\left(\frac{N}{v}x_1\cos\alpha\right)-\right.$$
$$\left.-\int_0^{\infty}d\beta K_0(\xi\,\mathrm{ch}\,\beta)f_1\left(\frac{N}{v}\mathrm{ch}\,\beta,y'\right)\sin\left(\frac{N}{v}x_1\,\mathrm{ch}\,\beta\right)\right\},\quad \xi=\frac{N}{v}|y-y'|. \tag{10}$$

For a source $f(r) = \delta(y)f_2(x,z) = \delta(y)f_2(-x,z)$ localized in the vertical plane the formula for the potential distribution in the plane of the source can be written in the form

$$\frac{\partial\psi}{\partial t}\Big|=\frac{m_0}{4\pi v}\int dz'\left\{\int_0^{\pi/2}d\alpha J_0(\zeta\sin\alpha)f_2\left(\frac{N}{v}\cos\alpha,z'\right)\sin\left(\frac{N}{v}x_1\cos\alpha\right)-\right.$$
$$-\int_0^{\pi/2}d\alpha N_0(\zeta\sin\alpha)f_2\left(\frac{N}{v}\cos\alpha,z'\right)\cos\left(\frac{N}{v}x_1\cos\alpha\right)- \tag{11}$$
$$\left.-\frac{2}{\pi}\int_0^{\infty}d\beta K_0(\zeta\,\mathrm{sh}\,\beta)f_2\left(\frac{N}{v}\mathrm{ch}\,\beta,z'\right)\sin\left(\frac{N}{v}x_1\,\mathrm{ch}\,\beta\right)\right\},\quad \zeta=\frac{N}{v}|z-z'|.$$

Finally, for a source elongated only in the direction of its movement $f(r) = \delta(y)\,\delta(z)f_3(x)$, in the general expression for potential one integration remains

$$\psi=-\frac{m_0}{2\pi v}\int d\omega G^r\left(\frac{\omega}{v},y,z,\omega\right)f_3\left(\frac{\omega}{v}\right)e^{i\omega x_1/v}. \tag{12}$$

2. Pressure Field of Point Source

For the pressure field created by a horizontally moving point source $f(r-vt) = \delta(y)\,\delta(z)\,\delta(x-vt)$, from the preceding formulas (for example, (12)) we have the integral formula

$$p=\frac{im_0}{2\pi v}\int d\omega\,\omega(N^2-\omega^2)G^r\left(\frac{\omega}{v},y,z,\omega\right)e^{i\omega x_1/v}, \tag{13}$$

in which, in a general case, the integral cannot be expressed through simple special functions. However, the pressure distribution along the three axes of an orthogonal coordinate system moving with the source, one of which is vertical, whereas the other coincides with the axis of movement, can be expressed through cylindrical and kindred functions.

The formula for the pressure distribution along the y-axis is easily derived from (10), assuming $x_1 = 0$ and $f_1(x,y) = \delta(x)\,\delta(y)$:

$$p|_{z=x_1=0}=\frac{m_0N^2}{2\pi^2 v}\int_0^{\pi/2}d\alpha\sin^2\alpha K_0(2Y\cos\alpha)= \tag{14}$$

$$= \frac{m_0 N^2}{8\pi v} \{I_0(Y)K_0(Y)+I_1(Y)K_1(Y)\}, \quad Y \equiv \frac{N}{2v}|y|. \tag{14}$$

Here the nature of the dependence on dimensional parameters was simple and it is easily established from some dimensionality considerations. The number of significant dimensional parameters in the case of a point source is small (m_0, N, v) and for the distribution of pressure along any ray r we will have (the linearity for m_0 is related to the linearity of the examination)

$$p(r) = (m_0 N^2/v)F(R), \quad R = Nr/v. \tag{15}$$

Formula (14) shows that in a transverse horizontal direction the pressure decreases monotonically with increasing distance from the source and in the far zone there is an inverse proportionality to distance

$$p|_{z=x_1=0} \approx m_0 N/4\pi|y|, \quad |y| \gg v/N. \tag{16}$$

For a transverse vertical direction the precise formula for pressure follows from (11)

$$p|_{y=x_1=0} = -\frac{m_0 N^2}{4\pi v}\int_0^{\pi/2} d\alpha \sin^2\alpha N_0(2Z\sin\beta) = \tag{17}$$

$$= -\frac{m_0 N^2}{16v}\{J_0(Z)N_0(Z)-J_1(Z)N_1(Z)\}, \quad Z \equiv \frac{N|z|}{2v}$$

and in the distant zone is reduced to the simple result

$$p|_{y=x_1=0} \approx -(m_0 N/4\pi|z|)\sin\left(\frac{N}{v}|z|\right), \quad |z| \gg v/N. \tag{18}$$

The pressure field oscillates vertically with a linearly decreasing amplitude; the wavelength of the oscillations in the distant zone is equal to $2\pi N/v$.

In order to determine the pressure change along the axis of movement it is convenient instead of formulas (10), (11) to use formula (2), substituting into it a simple expression of Green's function for horizontal directions (see [12])

$$\frac{\partial G^r(r,t)}{\partial t}\Big|_{z=0} = -\frac{\theta(t)}{4\pi\sqrt{x^2+y^2}} J_0(Nt).$$

In the case of a horizontally moving point source we obtain

$$p|_{z=0} = \frac{m_0}{4\pi}\left(\frac{\partial^2}{\partial t^2}+N^2\right)\int_0^{\infty} d\tau \frac{J_0(N\tau)}{\sqrt{y^2+(x_1+v\tau)^2}}. \tag{19}$$

In the special case $x_1 = 0$ from this formula we obtain (14). At the limit $y \to 0$ different results follow in dependence on the sign on x_1.

Ahead of the moving source ($x_1 > 0$) for the pressure distribution we obtain the formula

$$p|_{y=z=0}=\frac{m_0}{4\pi v}\left(\frac{\partial^2}{\partial t^2}+N^2\right)S_{0,0}\left(\frac{Nx_1}{v}\right)=\frac{m_0N}{4\pi x_1}S_{1,1}\left(\frac{Nx_1}{v}\right), \tag{20}$$

in which by $S_{\mu,\nu}(X)$ is meant the Lommel function. In the distant zone, with $X \gg 1$, using the asymptotic form $S_{1,1}(X)\approx 1 + X^{-2} + \ldots$, we find that the pressure field has an attenuating character (compare (16), (18))

$$p|_{y=z=0}\approx m_0N/4\pi x_1, \quad x_1\gg v. \tag{21}$$

On the "wake" axis behind the point source ($x_1<0$, $y = z = 0$), as indicated by formula (19), the pressure becomes equal to infinity. This peculiarity of point sources was noted earlier in [14], where an approximate solution of the problem was analyzed.

3. Energy of Internal Waves Generated by a Moving Source

The energy equation follows from the initial system of equations. It can be written in integral form

$$\frac{\partial}{\partial t}\int_V d^3r\left(\frac{\mathbf{v}^2}{2}+\frac{g^2}{2N^2}\rho^2\right)+\int_{\Sigma_V} d\sigma\, pv=\int_V d^3r\, pm\equiv W.$$

In the case of stationary movement the first term in the equation becomes equal to zero and there is an equality between the energy flux of internal waves through the surface $\sum V$ and the work of a mass source during a unit time against the pressure which it creates in the volume V surrounded by this surface. Hereafter, for the purpose of simplification, we will compute the last integral W.

Taking (1), (5) into account, the expression for the energy loss of a uniformly moving source W can be written in the form of an expansion in frequencies and wave vectors

$$W=\frac{im_0^2}{(2\pi)^3}\int d^3k\, d\omega\omega(N^2-\omega^2)G^r(\mathbf{k},\omega)|f(\mathbf{k})|^2\delta(\omega-\mathbf{kv}).$$

Due to the evenness of the operator $\hat{L}$ (see (1), (3)) the function $G^r(k,\omega)$ is even with respect to the components of the wave vector, and as is easy to see, a nonzero contribution to W will be given only by its part odd with respect to frequency. Accordingly, in actuality in the formula for the energy loss

$$W=\frac{im_0^2}{16\pi^3}\int d^3k\, d\omega\omega(N^2-\omega^2)D(\mathbf{k},\omega)|f(\mathbf{k})|^2\delta(\omega-\mathbf{kv}) \tag{22}$$

we have the function $D(k,\omega) = G^r(k,\omega) - G^r(k, -\omega)$, which is related by the inverse Fourier transform to solution of the homogeneous equation D(r, t)

$$\hat{L}D(\mathbf{r},t)=0, \quad \Delta D|_{t=0}=0, \quad \Delta(\partial D/\partial t)|_{t=0}=\delta(\mathbf{r})$$

and has a simple explicit form (see [12])

$$D(\mathbf{k},\omega)=-2\pi i\,\mathrm{sgn}\,\omega\delta(\omega^2k^2-N^2k_x^2-N^2k_y^2). \tag{23}$$

This makes obvious the sense of W as the energy loss in the generation of waves since the δ-function characterizes some packet of free waves (D(r,t) is the solution of the homogeneous equation).

In the case of a point source all the integrations are removed due to the δ-functions and we have the externally simple result

$$W=m_0 p|_{x=vt}, \tag{24}$$

that is, the energy losses are proportional to pressure at the source site. The formulas in the preceding section indicate the infinity of this value. In such a case a number of problems (such as the order of magnitude of the limiting transitions and integrations) will need additional analysis. We note that with $y\to 0$, $z\to 0$ the the expressions for p in formulas (14), (17) have a logarithmic singularity, whereas the divergence in (20) with $x\to vt$ has a power-law character.

Now we will examine a very simple source with three-dimensional nonlocality, specifically, a spherically symmetric source ($f(k) = \mu(k)$). Using formulas (22), (23) for a source moving along the horizontal axis x, transforming to the spherical coordinates k, φ, θ ($k_x = k \sin\varphi \sin\theta$, $k_y = k\cos\varphi\sin\theta$, $k_z = k\cos\theta$) and carrying out simple integrations for the angles φ, θ due to the two δ-functions, we obtain

$$W=\frac{m_0^2}{2\pi^2}\int_0^{\pi} d\omega\sqrt{N^2-\omega^2}\int_{N/v}^{\infty} dk\frac{\mu^2(k)}{\sqrt{k^2v^2-N^2}}. \tag{25}$$

As a result, for the energy loss in a unit time on the generation of internal waves by a horizontally moving nonlocal source from (25) we have the simple general formula

$$W=\frac{m_0^2N^2}{8\pi v}\int_0^{\infty} d\beta\mu^2\left(\frac{N}{v}\operatorname{ch}\beta\right). \tag{26}$$

For a source of a special type $f(r) = \pi^{-3/2}\ell^{-3}\exp(-r^2/\ell^2)$ we have $\mu(k) = \exp(-k^2\ell^2/4)$, and the integral in (26) is expressed through the cylindrical function

$$W=\frac{m_0^2N^2}{16\pi v}\exp\left(-\frac{N^2l^2}{4v^2}\right)K_0\left(\frac{N^2l^2}{4v^2}\right), \tag{27}$$

which with a small and large value of the ratio of the source to the parameter of its nonlocality gives

$$W\approx\begin{cases}\dfrac{m_0^2N}{8l\sqrt{2\pi}}\exp\left(-\dfrac{N^2l^2}{2v^2}\right), & v\ll Nl,\\ \dfrac{m_0^2N^2}{8\pi v}\ln\left(\dfrac{v}{Nl}\right), & v\gg Nl.\end{cases} \tag{28}$$

From this result follows an important conclusion concerning the logarithmic divergence of energy losses at the limit of the point source ($\ell\to 0$). The infinity of the energy losses is typical in problems of wave generation by a moving point source. In particular, as is well known [13, 15], for the Cerenkov radiation of light waves by a moving point charge, if the dispersion of properties of the medium is not taken into account, this will be observed. In the case of internal waves considered here they have a strong dispersion also when N = const. However,

as can be seen from (25), the dispersion of waves during horizontal movement leads to the suppression of the contribution of long waves and does not change the logarithmic divergence of losses for a point source due to the contribution of short waves.

4. Generation Pressure for Spherically Symmetric Source

For an evaluation of the part of the pressure p_W which is associated with the field of waves generated by a moving source (gives a contribution to the energy loss on wave generation) it is necessary, as is clear from the preceding text, that in the general formulas the $G^r(k, \omega)$ be replaced by $1/2D(k, \omega)$. Then from (5) we obtain

$$p_w = \frac{im_0}{16\pi^3}\int d^3k\, d\omega\, \omega (N^2-\omega^2) D(\mathbf{k}, \omega) f(\mathbf{k}) e^{i\mathbf{k}r_1}\delta(\omega-\mathbf{kv}), \tag{29}$$

which for a horizontally moving spherically symmetric source after introduction of spherical coordinates, integration for angles and replacement of the variables $\omega = N \cos \alpha$, $k = (N/v)\mathrm{ch}\, \beta$ assumes the form

$$p_w = \frac{m_0 N^2}{2\pi^2 v}\int_0^{\pi/2} d\alpha \int_0^{\infty} d\beta\mu \left(\frac{N}{v}\mathrm{ch}\,\beta\right) C(\alpha, \beta)\sin^2\alpha, \tag{30}$$

$$C(\alpha, \beta) = \cos\left(\frac{Nx_1}{v}\cos\alpha\right)\cos\left(\frac{Ny}{v}\cos\alpha\,\mathrm{sh}\,\beta\right)\cos\left(\frac{Nz}{v}\sin\alpha\,\mathrm{ch}\,\beta\right).$$

Hence, in special cases along the y-, z-axes for a point source we will have precisely the same results as in (14), (17), that is, the generation pressure coincides with the total pressure. Such a coincidence will also be observed in a more general case. The difference between the total pressure and the generation pressure can be represented in an integral form, similar to (29), with the replacement of $1/2D(k, \omega)$ by the even (with respect to frequency) part of the function $G^r(k, \omega)$. If the source has a "forward-backward" symmetry, then with $x_1 = 0$ the integrand is odd (with respect to frequency) and the integral disappears. Accordingly, in the transverse plane of symmetry of the source the total pressure coincides with the generation pressure.

On the axis of movement there is no such coincidence of total pressure and generation pressure. As can be seen from (30), for a spherically symmetric source $p_W(-x_1, y, z) = p_W(x_1, y, z)_\infty$ and in particular,

$$p_w(x_1, 0, 0) = \frac{m_0 N}{4\pi x_1} J_1\left(\frac{Nx_1}{v}\right)\int_0^{\infty} d\beta\mu\left(\frac{N}{v}\mathrm{ch}\,\beta\right), \tag{31}$$

whereas the total pressure on the axis of movement of the point source, according to (20), is infinite when $x_1 < 0$ and assumes finite values when $x_1 > 0$.

We note in conclusion that the change from a point source to a combination of point sources in the form of a dipole does not do away with divergences and at the limit of a point source intensifies them. Moreover, the generation energy

remains infinite and for a source distributed along the axis of movement $f(r) = \nu(x)\,\delta(y)\,\delta(z)$

$$W = \frac{m_0^2}{2\pi^2}\int_0^N d\omega\sqrt{N^2-\omega^2}\,|\nu(\omega/v)|^2\int_{N/v}^{\infty}\frac{dk}{\sqrt{k^2v^2-N^2}}. \qquad (32)$$

In this case, as for a point source, there is a logarithmic divergence of the second integral in the case of large wave numbers (for short waves).

BIBLIOGRAPHY

1. Mei, C. C., Wu, T. Y., "Gravity Waves Due to a Point Disturbance in a Plane Free Surface Flow of Stratified Fluids," PHYS. FLUIDS, 7, No 8, pp 1117-1133, 1964.

2. Wu, T. Y., "Three-Dimensional Internal Gravity Waves in a Stratified Free-Surface Flow," ZAMM, 45, T194-T195, 1965.

3. Wu, T. Y., Mei, C. C., "Two-Dimensional Gravity Waves in a Stratified Ocean," PHYS. FLUIDS, 10, No 3, pp 482-486, 1967.

4. Miles, J. W., "Internal Waves Generated by a Horizontally Moving Source," GEOPHYS. FLUID DYNAMICS, 2, No 1, pp 63-87, 1971.

5. Sturova, I. V., "Plane Problem of Wave Movements Arising in a Stratified Fluid During Flow Around a Submerged Dipole," DINAMIKA SPLOSHNOY SREDY (Dynamics of a Continuous Medium), Izd. IG SO AN SSSR, No 15, pp 157-169, 1973.

6. Sturova, I. V., "Wave Movements Arising in a Stratified Fluid During Flow Around a Submerged Body," PMTF (Applied Mathematics and Technical Physics), No 6, pp 80-91, 1974.

7. Nikishov, V. I., Stetsenko, A. G., "Plane Internal Waves Arising in a Stratified Fluid During Flow Around a Source-Loss System," GIDROMEKHANIKA (Hydromechanics), Kiev, "Naukova Dumka," No 36, pp 66-70, 1977.

8. Sturova, I. V., "Internal Waves Generated by Local Disturbances in a Stratified Fluid," DINAMICHESKIYE ZADACHI MEKHANIKI SPLOSHNYKH SRED (Dynamic Problems of the Mechanics of Continuous Media), Izd. IG SO AN SSSR, No 35, pp 122-140, 1978.

9. Sturova, I. V., "Internal Waves Generated by Local Disturbances in a Linearly Stratified Fluid of Finite Depth," PMTF, No 3, pp 61-69, 1978.

10. Sturova, I. V., "Internal Waves Generated by Local Disturbances in a Two-Layer Stratified Fluid," IZV. AN SSSR, FAO (News of the USSR Academy of Sciences: Physics of the Atmosphere and Ocean), 14, No 11, pp 1222-1228, 1978.

11. Sturova, I. V., Sukharev, V. A., "Plane Problem of Wave Movements Arising in a Continuously Stratified Fluid During Flow Around a Submerged Body," IZV. AKAD. NAUK SSSR, MZhG (News of the USSR Academy of Sciences: Mechanics of Fluids and Gases), No 4, pp 148-152, 1978.

12. Gorodtsov, V. A., Teodorovich, E. V., LINEYNYYE VNUTRENNIYE VOLNY V EKSPONENTSIAL'NO STRATIFITSIROVANNOY IDEAL'NOY NESZHIMAYEMOY ZHIDKOSTI (Linear Internal Waves in an Exponentially Stratified Ideal Incompressible Fluid), Preprint No 114, Institute of Mechanical Problems USSR Academy of Sciences, 1978.

13. Ivanenko, D. D., Sokolov, A. A., KLASSICHESKAYA TEORIYA POLYA (Classical Field Theory), Gostekhteoretizdat, 1951.

14. Dokuchayev, V. P., Dolina, I. S., "Generation of Internal Waves by Sources in an Exponentially Stratified Fluid," IZV. AN SSSR, FAO (News of the USSR Academy of Sciences: Physics of the Atmosphere and Ocean), 13, No 6, pp 655-663, 1977.

15. Tamm, I. Ye., SOBRANIYE NAUCHNYKH TRUDOV (Collection of Scientific Works), Vol 1, Moscow, "Nauka," 1975.

5303
CSO: 1865/63

UDC 551.46

GENERAL CIRCULATION OF THE WORLD OCEAN

Leningrad OBSHCHAYA TSIRKULYATSIYA MIROVOGO OKEANA in Russian 1980 (signed to press 17 Jan 80) pp 2-5, 252-253

[Annotation, foreword and table of contents from book "General Circulation of the World Ocean", by V. A. Burkov, Gidrometeoizdat, 1800 copies, 254 pages]

[Text] Annotation. The book gives a description of general circulation in the world ocean. The author presents the physiographic conditions for development of general circulation of the world ocean, defines it, examines the mechanical and thermohaline factors exciting general circulation, gives a brief overview of water masses and their tracers, describes the field of masses in the world ocean, and sets forth the method for formulating schemes of movement from the surface to the bottom of the ocean. The materials used in the work are characterized.

Macroscale schemes of general horizontal circulation of surface, subsurface intermediate, intermediate, deep and bottom waters are analyzed and the vertical structure of currents and elements of vertical movements are considered.

The book characterizes individual links in the general circulation — ocean currents of different types: equatorial and tropical, monsoonal, easterly and westerly boundary currents in subtropical anticyclonic circulations.

The book is intended for scientific workers, graduate students and undergraduates.

Foreword. This book, "General Circulation of the World Ocean," is an attempt at formulation and physical interpretation of the three-dimensional macroscale field of movement in the world ocean.

Systematic descriptions of general circulation of the world ocean in monographs and textbooks on oceanology [24, 44, 75, 106, 114, 143] have been incomplete with respect to coverage of regions of the world ocean and to a considerable degree are outdated. Since the time of writing of these monographs the number of observations of the main oceanological characteristics (temperature, salinity, oxygen content, currents) has increased by several times, although their distribution over the surface of the world ocean and in time still remains nonuniform. The overwhelming number of observations are concentrated in the northern parts of the Atlantic and Pacific Oceans and within these sectors the observations are concentrated in the coastal regions. The central parts of the oceans and the antarctic waters are still poor in observations.

In order to form a picture of general circulation of the world ocean it is possible to use direct or indirect methods. The direct methods include a generalization of instrumental measurements of currents. However, there are still so few such measurements that in the coming decades there will be no possibility of recreating the pattern of movement of ocean waters on their basis. An exception in this respect is the surface layer of the world ocean, the scheme of currents for which can be constructed using data on drift and deflection of ships. Such maps have also been constructed before [132] and are included in the oceanographic manuals mentioned above. A map of surface currents based on data on the drift and deflection of vessels is also given in our monograph on the basis of the results of modern computations made by Steed [136]. The characterizations of movements in the water layer are given on the basis of indirect methods, that is, on the basis of the results of one of the diagnostic models developed by the author [14, 15], not using direct measurements of currents, but data on the wind and density of ocean water related to the components of current velocities by hydrodynamic equations.

But for the time being even indirect data are limited. And they are by no means adequate for constructing even one synoptic model of the world ocean, as is done for the atmosphere. At present indirect data can be used only in constructing the stationary circulation of the world ocean, generalizing all the observations made in the history of oceanology in the form of the mean long-term annual values of the characteristics, related to unit areas, which are selected in dependence on the scales of movement. Exactly this is done in this monograph. For circulation schemes at the scale of the entire ocean we used the mean long-term annual values of the characteristics averaged for 5° spherical trapezia. For individual regions of the world ocean it was possible to employ the mean long-term seasonal values, related to 1° "squares."

In the critical evaluation of the results, in this monograph extensive use is made of a comparison of the constructed circulation schemes and the distribution of oceanological characteristics, primarily temperature, salinity and the oxygen content, using as a point of departure the concept of a close relationship between the fields of these characteristics and the field of movement in a baroclinic ocean.

The first five introductory chapters give the principal parameters of the world ocean as a physiographic component of the planet, give some idea concerning stationary and nonstationary forms of movement of ocean waters and a detailed description of the external factors exciting circulation, their relative contribution to the resultant circulation, as well as an exposition of the method for computing general circulation and a brief description of the initial data.

Three large chapters give a systematic description, critical analysis and the basic results for the three-dimensional field of movement in the world ocean: horizontal circulation of surface, subsurface intermediate, intermediate, deep and bottom waters, elements of vertical movements and the vertical structure.

As a result of rather rough averaging the pattern of general circulation of the world ocean obtained by computations naturally has a schematic character, although it satisfies the perception of its principal characteristics. However, in order to

collate it with the real pattern the book is supplemented by a large special chapter entitled "Currents in the World Ocean." In this chapter, insofar as possible, a description is given of individual currents on the basis of unaveraged observations of one or more expeditions or on the basis of mean data, but matched with the spatial scale of a particular current. This chapter also gives instrumental observations in order to characterize, unfortunately, those few currents for which they have been made. Thus, the reader will find material on how to proceed from the generalized pattern of general circulation to really existing flows in the world ocean.

In conclusion, the principal conclusions from the work are presented.

This book continues and generalizes studies made earlier devoted to the general circulation of individual oceans: Atlantic [8], Indian [17, 66], Pacific [13, 14] and even the world ocean [20]. The latter study of the macroscale characteristics of circulation of waters in the world ocean was presented in a preliminary and concise form. Thus, our monograph reflects the sequence of the entire direction of investigation and generalization of general circulation in the world ocean.

Due to the limited volume of the book, except for the chapter "Currents in the World Ocean," preference is given to original text and original illustrations. Reviews of the literature on the development of concepts concerning general circulation of the world ocean have been omitted. The first five introductory chapters deal only with those problems which are necessary for exposition of the main theme. In the remaining chapters, devoted to general circulation, comparisons of the newly obtained results with those obtained earlier are also limited. The author hopes that the book will come into the hands of an adequately trained reader capable of comparing the information obtained earlier with the results in this book and will evaluate them successfully. Along the lines of emphasis on the exposition of new results the bibliography is kept relatively modest. However, it contains all the main sources relating to general circulation, although it makes no pretense to completeness with respect to ocean physics and dynamics. On the other hand, the chapter "Currents in the World Ocean" makes extensive use of the sources in the literature, drawing upon fresh and reliable observational data.

This work on general circulation of the world ocean did not begin from scratch. In this monograph the author uses accumulated knowledge both on the actual pattern of circulation and on its physical nature. A generalization of this information is accomplished in part in the first five chapters of the monograph, which also contain some original results obtained by the author. Accordingly, the conclusion of the book must be regarded as a brief summary of our ideas concerning general circulation of the world ocean as interpreted by the author.

The description of general circulation is limited to three large oceans: Atlantic, Indian and Pacific, although, to be sure, their antarctic sectors are included. The Arctic Ocean is not included in the book because the author has not investigated it himself and did not wish to present a compilation. However, the Arctic Ocean can be regarded as a mediterranean sea, not formally, but from an oceanological point of view. And there are four such large mediterranean seas in the world ocean: the

Mediterranean Sea, Caribbean Sea, seas of the Sunda Archipelago and the Arctic Ocean. In the author's opinion, physical oceanography of these mediterranean seas can be the subject of a separate book.

To be sure, without the assistance of the staff of the Institute of Oceanology imeni P. P. Shirshov USSR Academy of Sciences the author would not have been able to handle such an enormous volume of material as was necessary for describing and analyzing the general circulation of the world ocean. The collection, systematic arrangement and processing of data on temperature, salinity and currents is but a small part of the work, in which many specialists participated. The author expresses deep appreciation to them. Among them, the author especially wishes to note the direct and constant assistance of V. S. Fedorov, A. I. Kharlamov, I. G. Usychenko and Ye. G. Morozov, who assisted with computations on an electronic computer.

The author is also deeply appreciative to Corresponding Member USSR Academy of Sciences A. S. Monin and Corresponding Member USSR Academy of Sciences V. G. Kort for valuable comments on the work.

CONTENTS

5303
CSO: 1865/103

TERRESTRIAL GEOPHYSICS

COLLECTION OF ARTICLES ON GEOPHYSICAL PROBLEMS

Leningrad UCHENYYE ZAPISKI LENINGRADSKOGO ORDENA LENINA I ORDENA TRUDOVOGO KRASNOGO ZNAMENI GOSUDARSTVENNOGO UNIVERSITETA IMENI A. A. ZHDANOVA: VOPROSY GEOFIZIKI in Russian No 404, Issue 28, 1980 (signed to press 6 Feb 80) pp 2, 238-247

[Annotation and selected abstracts from collection "Problems in Geophysics", edited by G. V. Molochnov, professor, and A. S. Semenov, professor, Izdatel'stvo Leningradskogo universiteta, 714 copies, 248 pages]

[Text] Annotation. The collection contains articles written by specialists of the Department of Physics of the Earth of the Physics Faculty of Leningrad State University and specialists of the geophysical departments and laboratories of the Geology Faculty of Leningrad State University. The published articles give a thorough review of the status of the problem of tidal phenomena and it is shown that the latter can be used in obtaining information on the internal structure of the earth; a physical mechanism of change in the magnetic states of rocks is proposed; a number of problems involved in the analysis of models of the earth's conductivity, solution of the direct and inverse problems in magnetotelluric sounding in inhomogeneous media, solution of the inverse problem in magnetometry, use of variable electromagnetic fields in study of the sea, and also detection of the noise arising during the registry of long-period oscillations of the earth are considered.

The collection is intended for scientific specialists, graduate students, students in advanced courses concerned with study of physics of the earth and engineers specializing in geophysics.

SELECTED ABSTRACTS

UDC 660.38.550.8

MEASUREMENTS OF MAGNETIC SUSCEPTIBILITY OF ROCKS UNDER NATURAL CONDITIONS

[Abstract of article by Kudryavtsev, Yu. I., and Miklyayev, Yu. V.]

[Text] The authors examine examples of application of the method for measuring magnetic susceptibility of rocks under natural bedding conditions. The results of profile measurements of magnetic susceptibility are used in increasing the effectiveness of interpretation of magnetic field curves. On the basis of the distribution of magnetic susceptibility values at the surface of an intrusive formation it

is possible to discriminate individual mineral facies and zones of mylonitization, evaluate the degree and depth of near-contact changes, and establish the characteristics of the internal structure of intrusive bodies. 4 figures, 8 references.

UDC 550.832.8.08

VALIDATION OF APPARATUS FOR INDUCTION MEASUREMENTS OF MAGNETIC SUSCEPTIBILITY AND CONDUCTIVITY OF A MEDIUM

[Abstract of article by Kudryavtsev, Yu. I.]

[Text] The article gives a block diagram of an instrument for measuring magnetic susceptibility and conductivity of a medium and a circuit diagram of the probe. In the instrument provision is made for stabilizing the amplitude of the magnetic moment of the generating coil, the reference and compensating voltages, regardless of the effect of the investigated medium. In addition, a constant phase ratio is maintained between the magnetic moment and the reference and compensating voltages, as well as the measured emf. As a result, there is an increase in accuracy, phase selectivity and response of the measurements. 2 figures, 9 references.

UDC 550.835.002.56

ROENTGENORADIOMETRIC SENSORS WITH TWO-STAGE EXCITATION FOR THE TESTING OF ORES IN MINE WORKINGS AND IN BOREHOLES

[Abstract of article by Meyer, V. A., Nakhabtsev, V. S., Ivanyukovich, G. A., and Krotkov, M. I.]

[Text] The authors describe the design and characteristics of sensors for the testing of ores developed at Leningrad State University. In the sensors for the excitation of fluorescence of the elements to be determined use is made of the secondary emission of the target, which, in turn, is excited by a radioisotope source. Provision is also made for the use of the primary emission of the source for irradiation of the investigated medium. The use of two-stage excitation makes it possible to enhance the response and selectivity of roentgenoradiometric analysis. 4 figures, 5 references.

UDC 550.831(075.8)

DETERMINATION OF THE PARAMETERS OF AN OBLIQUE THIN STRATUM FROM GRAVITY ANOMALIES

[Abstract of article by Mironov, V. S.]

[Text] A geometrical method is proposed for determining the parameters of an oblique material band from its gravity anomalies. This method can also be used in determining the parameters of strata with an infinite extent in depth on the basis of anomalies of the gravity gradient.

UDC 550.834.24

LOW-VELOCITY INTERFERENCE WAVES IN SEISMIC PROSPECTING. I. SURFACE WAVES

[Abstract of article by Rudakov, A. G.]

[Text] The article gives an analysis of the problem and methods for studying low-velocity interference waves in different stages of development of seismic prospecting by the reflected waves method. The author gives a substantiation of the need for a new approach to study of waves of this class in connection with a universal changeover to modifications of multiple overlappings in the common deep point method. In the first (published) part of the article the emphasis is on surface waves: their characteristic properties (range of apparent velocities, apparent periods, positions in the plane of the travel-time curve), the patterns of correlation of these properties with the properties of high-frequency registry, and also existing concepts concerning the nature of waves of this type. 4 figures, 45 references.

UDC 550.312;528.27;528.56

TIDAL PHENOMENA

[Abstract of article by Lin'kov, Ye. M.]

[Text] An investigation of tidal phenomena, such as earth and ocean tides, tidal changes of the rate of the earth's rotation, tidal friction, etc., is a vigorously developing field of terrestrial physics. The article reflects virtually all aspects of this interesting and important problem. Russian and Soviet geophysicists have made a major contribution to solution of this problem. The article gives a description of tidal phenomena and formulates the basic principles in the statistical theory of tides. The Laplace method is examined and the characteristics of the principal tidal waves and the dependence of their theoretical amplitudes on latitude are considered. The basic principles of the Love theory are given, illustrating the possibility of determining Love numbers from tidal phenomena. Experimental results of determination of Love numbers are also given. Also considered is a method for taking into account the influence of ocean tides on earth tides. The influence of inertial accelerations on gravimeter readings is also evaluated. The nature of tidal friction and its role in secular slowing of the earth's rotation is described. The influence of earth and ocean tides on secular slowing of the earth's rotation is considered. In conclusion, the results of investigations of tidal phenomena are summarized. 12 figures, 3 tables, 40 references.

UDC 550.830:519

INFORMATION CONTENT OF COMPONENTS OF THE MAIN COMBINATIONS OF SECONDARY CRITERIA IN DISCRIMINANT PROBLEMS IN MAGNETOMETRY

[Abstract of article by Zhezhel', N. F., and Zhezhel', Yu. N.]

[Text] The authors discuss methods for evaluating the information content of secondary criteria in interpretation problems related to determination of the qualitative state of the investigated object or medium. It is shown that for practical

purposes instead of evaluations of the information content of criteria considered separately it is desirable to use evaluations of the probability of the occurrence of the analyzed criteria in different effective groups, averaged for a series of problems. 4 figures, 2 tables, 3 references.

UDC 550.837.6

DETERMINATION OF THE DEPTH OF A CONDUCTING LAYER FROM THE RESULTS OF MAGNETOTELLURIC SOUNDING IN MEDIA CONTAINING SURFACE INHOMOGENEITIES

[Abstract of article by Porokhova, L. N., and Pogareva, O. I.]

[Text] The paper gives the results of interpretation of two model sections complicated by inhomogeneities of the bench type and the graben-bench-horst type with a horizontally polarized field using statistical interpretation algorithms developed for horizontally layered media. It is shown that the joint interpretation of the complex of curves on the profile, complicated by horizontal inhomogeneities causing the "S effect," makes possible a quite precise determination of the parameters of the conducting layer without recourse to complex solutions of the direct problem. 4 figures, 1 table, 3 references.

UDC 550.837.61

ELECTROMAGNETIC FIELD OF THE VERTICAL HARMONIC MAGNETIC DIPOLE AT THE SEA-BOTTOM DISCONTINUITY

[Abstract of article by Molochnov, G. V., Katkov, V. N., and Radionov, M. V.]

[Text] In this article numerical data are used in an analysis of the behavior of the electromagnetic field of a harmonic magnetic dipole situated at the sea-bottom discontinuity. Cases of different conductivity of the sea floor are examined. 1 figure, 1 reference.

UDC 550.34

SPECTRAL COMPOSITION AND NOISE LEVEL ON RECORDS OF A LONG-PERIOD SEISMOMETER

[Abstract of article by Petrova, L. N., and Lepeshkin, F. G.]

[Text] The mean spectra of seismic noise and microvariations of atmospheric pressure in the range 10-60 minutes are given. The authors give comparisons of the spectra of seismic oscillations and magnetic field variations, as well as the levels of spectral amplitudes of noise and long-period seismic oscillations (useful signal). The conclusion is drawn that in the absence of a useful signal the seismic record to a considerable degree is a result of changes in atmospheric pressure on the instrument and soil. No influence of magnetic field variations on seismometer readings was discovered. Noise data make it possible to correct the

spectra of long-period oscillations, and accordingly, determine their parameters more precisely. 2 figures, 4 references.

UDC 550.837.6

BEHAVIOR OF MAGNETOTELLURIC SOUNDING CURVES IN COASTAL REGIONS ON THE BASIS OF THE RESULTS OF MODELING

[Abstract of article by Dobrovol'skaya, M. A., Kovtun, A. A., and Kokvina, Ye. D.]

[Text] Magnetotelluric sounding curves near several types of characteristic sea sections (in a model) are examined. The behavior of these curves is analyzed as a function of the distance of the sounding point to the boundary of the inhomogeneity and the depth of the sounding point. As a result of the analysis some recommendations are given on carrying out magnetotelluric soundings in the coastal regions. 3 figures, 5 references.

UDC 550.837

USE OF THE SLOPE OF THE MAJOR AXIS OF THE MAGNETIC FIELD POLARIZATION ELLIPSE IN FREQUENCY SOUNDING

[Abstract of article by Molochnov, G. V., Radionov, M. V., Seku, Konate]

[Text] The author examines the possibilities of carrying out frequency soundings with measurement of the slope of the major axis of the polarization ellipse of a vertical magnetic dipole to the horizon α. On the basis of an analysis of the computations a study was made of the behavior of the angle over two-layer media with poorly and well-conducting bases. The effective characteristic $\tilde{\rho}/\rho_1(\tilde{h}/h_1)$ is introduced. The dependence of effective resistivity on the effective depth of penetration of the electromagnetic field is given; it is simple and convenient to use in interpretation. An investigation of the behavior of the $\tilde{\rho}/\rho_1(\tilde{h}/h_1)$ curves made it possible to develop isoparametric frequency-distance soundings in the zone of mean parameters. 4 figures, 11 references.

BAROVARIATIONS AS NOISE IN LONG-PERIOD SEISMIC OBSERVATIONS

[Abstract of article by Kozhevnikova, E. G., Orlov, Ye. G., and Lin'kov, Ye. M.]

[Text] The article describes the design of a microbarograph with a magnetron converter, methods for calculating the characteristics of the pressure elements and calibration of a concentrated load. The spectra of barovariations in the range of periods 200-5000 sec are given. 2 figures, 7 references.

5303
CSO: 1865/104

UDC 550.837

INTERPRETATION OF LOCAL GEOMAGNETIC ANOMALIES BY THE 'CONTRACTING SURFACES' METHOD

Novosibirsk GEOLOGIYA I GEOFIZIKA in Russian No 12, Dec 80 pp 106-117

[Article by M. S. Zhdanov and I. M. Varentsov, Institute of Terrestrial Magnetism, Ionosphere and Radio Wave Propagation, Troitsk, Moscow Oblast, manuscript submitted 21 Sep 79]

[Text]

Abstract: The author proposes an iteration algorithm for determining the form of a local deep geoelectric inhomogeneity situated in a layered medium under the condition that the parameters of the layers (their conductivity and thickness), and also the excess conductivity of the inhomogeneity are known. The form of the inhomogeneity is determined in the process of minimizing the functional of the mean square deviation between the observed and model fields. The minimizing problem is solved by the gradient method. The described algorithm is applied in the form of a program in FORTRAN-IV language, intended for the interpretation of two-dimensional E-polarized fields.

The most important problem involved in modern methods of geoelectric exploration is a study of anomalies of the variable geomagnetic field caused by horizontal inhomogeneities of the geoelectric section. As is well known, geomagnetic anomalies, in accordance with the nature of the sources causing them, can be divided into two groups: surface and deep [2, 9, 10, 15]. The first group includes anomalies associated with inhomogeneity of the surface layer of the earth's crust; the second are anomalies caused by deep inhomogeneities in the earth's crust and upper mantle.

In most cases the interpretation of surface anomalies essentially involves a determination of the total longitudinal conductivity of the surface inhomogeneous layer of the earth, which can be done using integral transforms of the observed field [10, 11, 16, 20, 21].

The problem of interpretation of deep geomagnetic anomalies is more complex. The author of [9] proposes a method for its solution based on an analytical continuation of the field into the lower half-space. An analysis of the vector lines of

the analytically continued electromagnetic fields in some situations of practical importance makes it possible to determine the position and form of deep inhomogeneities [23].

For a more detailed determination of the configuration of deep geoelectric inhomogeneities it is desirable to employ the ideas of the trial and error method, widely employed in different geophysical investigations and making it possible to correct the configuration of the region with anomalous conductivity on the basis of a comparison of the theoretically computed fields and the results of practical observations. This article is devoted to further development of these methods.

Formulation of Problem

We will examine a two-dimensional model of the geoelectric section consisting of a conducting horizontally layered earth with z = 0 in contact with a homogeneous nonconducting atmosphere. The conductivity (σ_n, n = 1, N) and the thickness (h_n, n = 1, N - 1, $h_N = \infty$) of the layers in the model are assumed to be known. Assume that in the earth there is a geoelectric inhomogeneity Q characterizing a conductivity different from a normal distribution:

$$\sigma(\bar{r}_q) = \begin{cases} \sigma_n, & r_q \notin Q \\ \sigma_n + \Delta\sigma(\bar{r}_q), & \bar{r}_q \notin Q. \end{cases} \quad (1)$$

Here $\bar{r}_q$ is the radius-vector of the observation point and $\Delta\sigma(\bar{r}_q)$ is an arbitrary function describing anomalous conductivity.

The field is excited by extraneous electrical currents distributed in the P region of the atmosphere. The dependence of the field on time is expressed by means of the factor $e^{-i\omega t}$. The permeability in the entire space is constant and equal to $\mu_0 = 4\pi \cdot 10^{-7}$ H/m. We will neglect displacement currents. We will assume that the field and medium are homogeneous along the y-axis, that is, we will solve the problem in a two-dimensional formulation. We will limit ourselves to examination of the most interesting case of E-polarization.

Assume that in this model we know the synchronous values of the magnetic field $\bar{H}$ on some profile L on the earth's surface in the range of frequencies Ω, the parameters of the normal geoelectric section $\{\sigma_n, h_n\}$ and the form of the functional dependence of anomalous conductivity $\Delta\sigma$ on the coordinates of the observation point. The problem is to determine the boundary of the region Q characterizing this anomalous conductivity.

In formulating the problem the question naturally arises as to the uniqueness of its solution. In the theory of potential fields the answer to this question is given by the Novikov theorem [13], guaranteeing uniqueness of solution of the inverse problem for stellate bodies with a known distribution of excess density. In the theory of electromagnetic fields there is no such theorem and therefore the problem, in essence, is to find one of the possible solutions (the inverse problem is formulated in a similar way in the method proposed by Weidelt [21]). In addition, under the condition that the electromagnetic fields are measured on some extensive profile on the earth's surface in some range of periods, there is every basis for assuming that this information is adequate for an unambiguous determination of deep inhomogeneities. In particular, P. Weidelt demonstrated the uniqueness

of solution of the inverse problem for the case when the conductivity of the section is described by an analytical function [22].

In solving the formulated problem by the trial and error method it is necessary to compare the observed fields with the results of numerical computations. A rigorous solution of the direct problem for the region of any inhomogeneity of a quite arbitrary configuration requires an examination of rather complex systems of integro-differential (or finite difference) equations [6, 7, 18, 19, 21]. Accordingly, in formulating effective trial and error algorithms it is desirable to use simpler approximate approaches to solution of direct problems. In particular, in some situations with a relatively small extent of the region Q in comparison with the wave length a sufficiently precise approximation can be obtained if in solution of the integral equations by the "contracting images" method we limit ourselves to the first iteration [3, 5, 7, 12]. Physically this means that we stipulate the excess currents j_{ex} induced in the region of the inhomogeneity Q, proportional to the normal electric field. In particular, with E-polarization

$$\bar{j}_{ex} = (0,\ j_{ex},\ 0),$$

and the scalar function f_{ex} can be approximately determined using the formula

$$j_{ex} = \Delta\sigma E_y^n, \tag{2}$$

where E_y^n is the normal electric field.

The distribution of the normal electric field E_y^n in a layered earth is determined by well-known methods [1, 8, 23] by analytical continuation of the normal component of the electric field, discriminated from the observed field at the surface, within the earth. Thus, the inverse problem in the analysis of deep anomalies is reduced to the finding of the boundary of the region Q characterizing the distribution of excess conductivity $\Delta\sigma$. The excess currents flowing in the Q region can be considered as extraneous currents exciting the deep anomalous field. Accordingly, the problem involves determination of the configuration of the Q region filled with extraneous currents of a known density.

We note, finally, that in a theoretical investigation of the formulated problem it is convenient to operate not with the magnetic field $\bar{H}$ itself, but its flux function Ψ, which in the region of homogeneity of the medium unambiguously determines the components of the electromagnetic field: $H_x = \partial\Psi/\partial z$, $H_z = -\partial\Psi/\partial x$, $E_y = -i\omega\mu_0\Psi$.

Determination of the Boundary of the Region Filled With Excess Currents

Assume that we know the flux function $\hat{\Psi}$ of a deep anomalous field on some profile L on the earth's surface in the range of frequencies Ω. In addition, we know the density distribution of the "extraneous" excess currents j_{ex} flowing in the region $\hat{Q}$, whose boundary is to be determined.

Henceforth we will assume that this region is stellate relative to some internal point O, whose coordinates are stipulated. At the point O we place the origin of a polar system of coordinates (ρ, φ) and we describe the boundary of the $\hat{Q}$ region in these coordinates by the equation

$$\rho = \hat{f}(\varphi).$$

The problem is as follows: on the basis of the known function $\hat{\Psi}$, find the boundary of the anomalous region $\hat{Q}$, that is, determine the unknown function $\hat{f}(\varphi)$.

We will limit ourselves to finding the function $\hat{f}$ describing the boundary of $\hat{Q}$ in the class of continuous functions F:

$$F = \{f(\varphi) : f(\varphi) > 0,\ f(\varphi + 2\pi) = f(\varphi),\ -\pi \leqslant \varphi \leqslant \pi\}.$$

Each function f from F in polar coordinates fixes the boundary ∂Q_f of some region Q_f. The flux function of the corresponding magnetic field, excited by the currents j_{ex}, flowing in the region Q_f, is determined in the following way:

[и36 = ex]
$$\Psi_f(\bar{r}) = \int_{-\pi}^{\pi}\int_{0}^{f(\bar{\varphi})} j_{изб}(\bar{r}^m)\, G_n(\bar{r}, \bar{r}^m)\, \rho d\rho d\varphi, \tag{3}$$

where $G_n(\bar{r}, \bar{r}^m)$ is the Green's function of a layered (normal) section, and $\bar{r}^m$ is the radius-vector of the current integration point $m \in Q_f$ with the coordinates (ρ, φ).

For effective solution of the direct problem we will examine a representation of Green's function in the form of the Fourier integral

$$G_n(\bar{r}\ \bar{r}^m) = G_n(x, z; \bar{r}^m) = \frac{1}{2\pi}\int_{-\infty}^{\infty} g_n(k_x, z; \bar{r}^m)\, e^{-ik_x \cdot x} dk_x,$$

in which the spectral density g_n (k_x, z, $\bar{r}^m$) is expressed relatively simply through the elementary functions [21], and it can be computed using an economical FFT (fast Fourier transform) algorithm. After transposition of the Fourier transform operation and integration in (3), we obtain a formula which is simpler from the computational point of view

[и36 = ex]
$$\Psi_f(\bar{r}) = \Psi_f(x, z) = \frac{1}{2\pi}\int_{-\infty}^{\infty} e^{-ik_x \cdot x}\int_{-\pi}^{\pi}\int_{0}^{f(\varphi)} j_{изб}(\Sigma\bar{r})\, g_n(k_x, z; \bar{r}^m)\, \rho d\rho d\varphi dk_x. \tag{3a}$$

In the class F we will seek such a function $\tilde{f}$ for which the corresponding flux $\Psi_{\tilde{f}}$ is sufficiently close (in some metrics) to the flux function $\hat{\Psi}$ of the field stipulated at the earth's surface. The measure of closeness of the observed and theoretically computed fields for simplicity will be taken in the metrics of the complex space $L_2[\omega, x]$:

$$\|\Psi\| = \sqrt{\int_{\Omega}\int_{L} |\Psi|^2 dx d\omega} = \sqrt{\int_{\Omega}\int_{L} \Psi \cdot \Psi^* dx d\omega}, \tag{4}$$

where the asterisk denotes a complexly conjugate value, Ω and L are the interval of frequencies and the observation profile, for which the Ψ function is known.

Thus, the problem is to find such a function $\tilde{f}$ for which

$$\|\Psi_{\tilde{f}} - \hat{\Psi}\| \leqslant \varepsilon_0 \|\hat{\Psi}\|, \tag{5}$$

where ε_0 is the required relative approximation error, determined by the accuracy δ in stipulating the initial data.

In solving the problem of the choice of the function $\hat{f}_i$ we will construct the following iteration process. Assume that we know some approximation f_i to the function $\hat{f}$. We will seek the (i + 1)-st approximation from the condition:

$$\|\Psi_{f_{i+1}} - \hat{\Psi}\| < \|\Psi_{f_i} - \hat{\Psi}\|.$$

If we introduce the quadratic functional I[f] into consideration

$$I[f] = \|\Psi_f - \hat{\Psi}\|^2, \tag{6}$$

the condition (5a) is written in the form

$$I[f_{i+1}] < I[f_i]. \tag{7}$$

Thus, we will construct a series of functions $\{f_i,\ i = 0, 1, 2, \ldots\}$ minimizing the functional I.

Here it must be noted that the problem to be solved, like most inverse problems in geoelectrics, is incorrectly formulated. Accordingly, the direct minimizing of the functional I, complicated by errors in observation and computations, can be reduced to unstable, geologically meaningless results. In order to obtain stable results it is necessary to apply the methods for regularization of incorrectly formulated problems. We will seek a regularized solution of the problem of choosing the configuration of a deep geoelectric inhomogeneity by minimizing the A. N. Tikhonov parametric functional [17]:

$$M_\alpha[f] = I[f] + \alpha\Omega[f] \tag{8}$$

with a corresponding value of the regularization parameter $\alpha = \alpha(\delta)$. The stabilizing functional $\Omega[f]$, conforming to [4], is stipulated in the form

$$\Omega[f] = \|f - f_0\|^2 = \int_{-\pi}^{\pi} (f - f_0)^2 d\varphi, \tag{9}$$

where f_0 is the initial approximation from the class F, stipulated on the basis of a priori geological-geophysical information.

We will construct the iteration process of minimizing the functional M_α with a fixed value of the α parameter. The common term of the minimizing sequence $\{f_i\}$ will be examined in the form

$$f_{i+1}(\varphi) = f_i(\varphi) + t_{f_i} \cdot g_{f_i}(\varphi),\ i = 0, 1, 2, \ldots \tag{10}$$

Here $g_{fi}(\varphi)$ are the functions of the increments, determined in the class of continuous functions G: $G = \{g(\varphi) : g(\varphi + 2\pi) = g(\varphi),\ -\pi \leqslant \varphi \leqslant \pi\}$

with the uniform metrics $\|g\| = \max_{-\pi < \varphi < \pi} |g(\varphi)|$,

t_{fi} is some set of positive constants, denoting the value of the approximation intervals. If the constants t_{fi} are sufficiently small, the functions f_i, the same as f_0, belong to the class F.

We will compute the functional $M\alpha$ for the function f_{i+1}. Due to the differentiability of this functional, the following representation is correct:

$$M_\alpha[f_{i+1}] = M_\alpha[f_i] + t_{f_i} M_\alpha^{(1)}[f_i, g_{f_i}] + t_{f_i}^2 \bar{o}(\|g_{f_i}\|), \tag{11}$$

in which $M_{\alpha}^{(1)}[f_i, g_{f_i}]$ is the first variation of the functional M_{α}, determined by the expression

$$M_{\alpha}^{(1)}[f_i, g_{f_i}] = \lim_{t_{f_i} \to 0} \frac{1}{t_{f_i}} \{M_{\alpha}[f_i + t_{f_i} g_{f_i}] - M_{\alpha}[f_i]\} =$$

$$= +2 \int_{-\pi}^{\pi} g_{f_i} \left\{ f_i \int_{\Omega} \mathrm{Re} \left(j_{\text{изб}}(\bar{r}_{f_i}) \int_{L} [\Psi_{f_i} - \hat{\Psi}]^{*} G_n(\bar{r}, \bar{r}_{f_i})\, dx \right) d\omega + \alpha (f_i - f_0) \right\} d\varphi, \tag{12}$$

where $\bar{r}_{f_i}$ is the radius-vector of the point with the coordinates $(f_i(\varphi), \varphi)$.

Equation (11) shows that with sufficiently small t_{j_i} the minimizing condition

$$M_{\alpha}[f_{i+1}] < M_{\alpha}[f_i] \tag{13}$$

is satisfied as soon as

$$M_{\alpha}^{(1)}[f_i, g_{f_i}] < 0. \tag{14}$$

In order to satisfy the latter condition it is sufficient to stipulate the function of increments g_{f_i} in the form

$$g_{f_i} = -|h_{f_i}|^{\beta} \operatorname{sign} h_{f_i}, \tag{15}$$

where

$$h_{f_i} = +f_i \int_{\Omega} \mathrm{Re} \left(j_{\text{изб}}(\bar{r}_{f_i}) \int_{L} [\Psi_{f_i} - \hat{\Psi}]^{*} G_n(\bar{r}, \bar{r}_{f_i})\, dx \right) d\omega + \alpha (f_i - f_0),$$

[Изб = ex]

$$\beta = \text{const} \geqslant 0. \tag{16}$$

With such a determination of the function g_{f_i} the first variation of the functional M_{α} is equal to

$$M_{\alpha}^{(1)}[f_i, g_{f_i}] = -2 \int_{\pi}^{\pi} |h_{f_i}|^{1+\beta} d\varphi \leqslant 0, \tag{17}$$

from which it follows that the inequality (14) is satisfied provided that $h_{f_i} \not\equiv 0$ (and accordingly, $g_{f_i} \not\equiv 0$).

For determining the t_{f_i} value we will examine the function

$$\Phi(t) = M_{\alpha}[f_i + g_{f_i}]$$

and we will seek t_{f_i} from the minimum condition $\Phi(t)$. For sufficiently small t a minimum always exists due to the negative value of the first variation of the functional M_{α} and formula (11). The problem of one-dimensional minimizing is solved by standard methods [14].

The formulas (10)-(15) make it possible, proceeding on the basis of some initial approximation $f_0 \in F$ and the initial interval t_{f_0}, to construct a series of functions $\{f_i\}$ minimizing the functional M_{α}. These functions in space describe cylindrical surfaces contracting toward the surface of the anomalous region $\hat{Q}$. Accordingly, the proposed method was given the name "contracting surfaces method."

The described iteration process with a fixed α parameter is completed under the condition

$$\|f_i - f_{i-1}\| \leqslant \varepsilon_1, \tag{18}$$

where $\varepsilon_1 > 0$ is some stipulated value. The optimum value of the regularization parameter α is selected from the series $\{\alpha_p\}$, converging to zero,

$$\alpha_{p+1} = \mu\alpha_p, \quad p = 1, 2, \ldots; \quad 0 < \mu < 1. \tag{19}$$

For each value of the parameter $\alpha = \alpha_p$ there is a minimizing of the functional $M_{\alpha_p}[f]$ by the described scheme. The result of the minimizing -- the function f_{α_p} -- is used as an initial approximation for minimizing the functional $M_{\alpha_{p+1}}[f]$ (for the functional $M_{\alpha_1}[f]$ the initial approximation is the function f_0). As the quasioptimum regularization parameter α_{qo}, for which the corresponding function of the series $\{f_{\alpha_p}\}$ is closest to the precise solution of the problem f, we select, conforming to [4], the parameter α_{qo}, for which there is satisfaction of the condition

[KO = qo = quasioptimum]

$$\sigma(\alpha_{ko}, \delta) = \min_p \|f_{\alpha_{p-1}} - f_{\alpha_p}\|. \tag{20}$$

The function $\tilde{f} = f_{\alpha_{qo}}$, corresponding to the parameter α_{qo}, is a quasioptimum approximation to the f solution.

Spectral Modification of Method

The computation scheme for the "contracting surfaces method" can be simplified by proceeding to an analysis of the spatial spectra of the observed electromagnetic fields. Assume that in some range of space frequencies $K = (k'_x, k''_x)$ we know the function $\hat{\Psi}$ -- the Fourier transform along the x axis of the flux function Ψ, considered above,

$$\hat{\psi}(k_x, z) = F_x[\Psi(x, z)] = \int_{-\infty}^{\infty} \Psi(x, z) e^{ik_x \cdot x} dx.$$

The "spectral" direct problem $\psi_f = F[\Psi_f]$ is solved using a formula following from (3), (3a):

[изб = ex]

$$\psi_f(k_x, z) = \int_{-\pi}^{\pi} \int_0^{f(\varphi)} j_{изб}(\bar{r}^{\prime\prime}) g_n(k_x, z; \bar{r}^{\prime\prime}) \rho d\rho d\varphi. \tag{21}$$

The latter formula no longer contains the Fourier transform operation; therefore, the volume of the computations is substantially reduced.

We will examine the quadratic functional

$$\mathcal{J}[f] = \|\psi_f - \hat{\psi}\|^2, \tag{22}$$

determining the measure of closeness of the Fourier transforms of the observed and computed fields, in the metrics of the complex space $L_2[\omega, k_x]$:

$$\|\psi\| = \sqrt{\int_{\pi} \int_{K} |\psi|^2 dk_x d\omega} = \sqrt{\int_{\Omega} \int_{K} \psi\psi^* dk_x d\omega}. \tag{23}$$

A comparison of expressions (22), (23) with (4), (6) reveals a great similarity between the functional I[f] and its spectral analogue $\mathcal{J}[f]$. Moreover, in the special situation when $L = (-\infty, \infty)$ and $K = (-\infty, \infty)$ these functionals are equal due to the well-known Parseval equation. Therefore, for solving the problem

of minimizing the $\mathcal{J}$ functional it is natural to use the regularizing procedure described above. In this case it is necessary only to replace I[f] in formulas (8)-(20) by $\mathcal{J}[f]$, Ψ by Ψ^{δ}, $x \in L$ by $k \in K$, G_n by g_n.

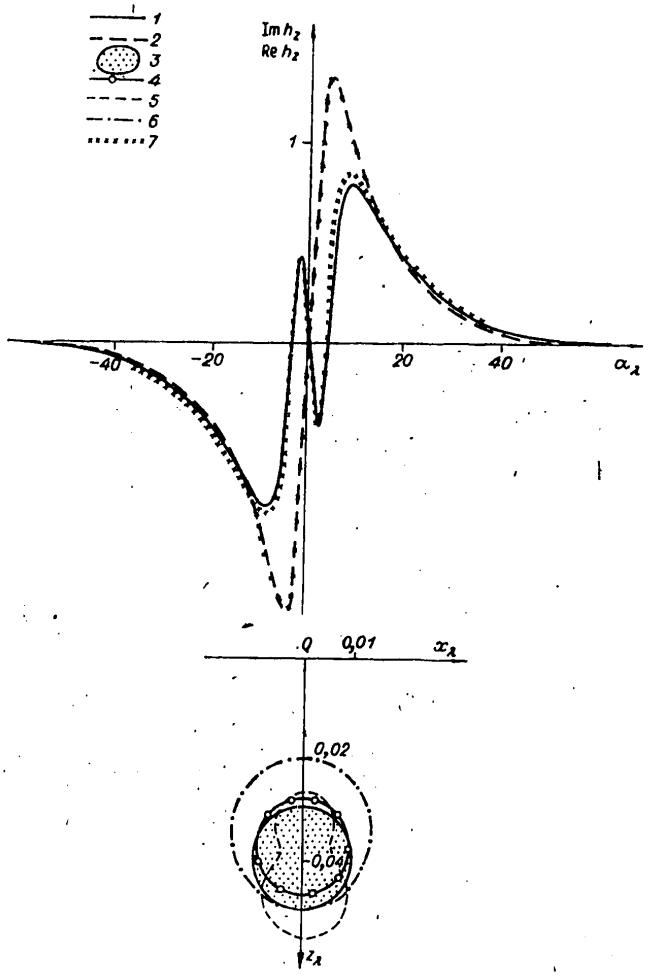

Fig. 1. Determination of form of conducting circular cylinder by the "contracting surfaces method." 1, 2) curves of real and fictitious parts of spectrum of vertical component of magnetic field $\hat{h}_z$ at earth's surface; 3) boundary of cylindrical inclusion; 4) result of solution of inverse problem with regularization; 5) same, without regularization; 6) initial approximation; 7) values Re h_z, Im hz, computed for model 4; specific conductivities of inclusion σ_I and surrounding medium σ_E (and so forth in figures).

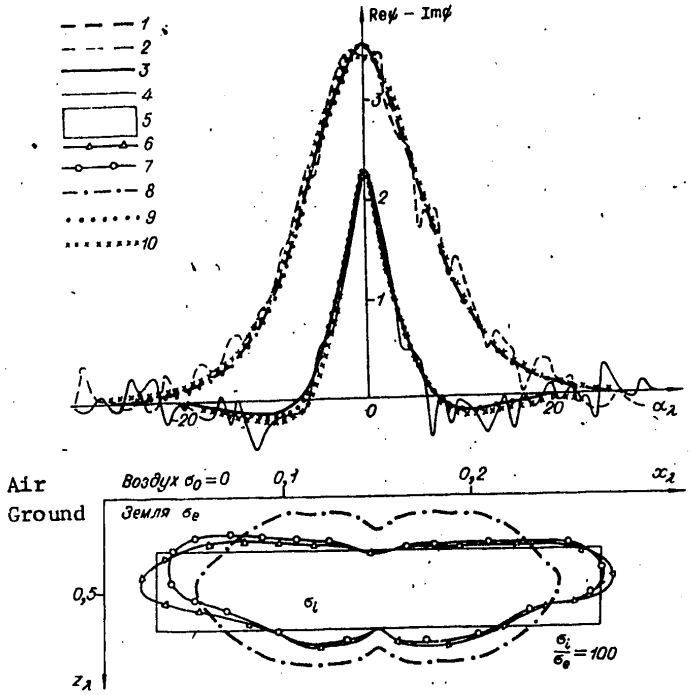

Fig. 2. Determination of configuration of rectangular inclusion of anomalous conductivity by "contracting surfaces method." 1, 3) curves of real and fictitious parts of spectrum of flux function $\hat{\Psi}$ of magnetic field at earth's surface; 2, 4) same curves, complicated by 10% error; 5) boundary of rectangular inclusion; results of solution of inverse problem; 6) according to precise data; 7) according to approximate data; 8) initial approximation; 9) values Re ψ, Im ψ, computed for model 6; 10) same for model 7.

Examples of Interpretation of Deep Anomalies by "Contracting Surfaces Method"

On the basis of a spectral modification of the "contracting surfaces method" the INEMTA program, written in FORTRAN-IV language and applied on a YeS-1010 electronic computer, was developed. It makes it possible to carry out an interpretation of anomalies of two-dimensional E-polarized fields (H_x, H_z, E_y, Ψ) on the basis of the corresponding space spectra.

The program was tested in a number of models of deep electromagnetic anomalies. The first example (Fig. 1) illustrates the need for using regularizing algorithms in determining the configuration of deep geoelectric inhomogeneities. The model consists of a homogeneous earth containing an anomalous region in the form of a horizontal circular cylinder. The solution of the inverse problem, without regularization ($\alpha = 0$) leads to a result differing greatly from the true configuration of the inhomogeneity. The standard deviation of the spectrum of the observed field

from the theoretically computed field for the model obtained in the course of solution of the inverse problem of the model is only 2%, which indicates a high degree of instability of the problem. At the same time, the use of a regularizing algorithm makes it possible to obtain entirely satisfactory results.

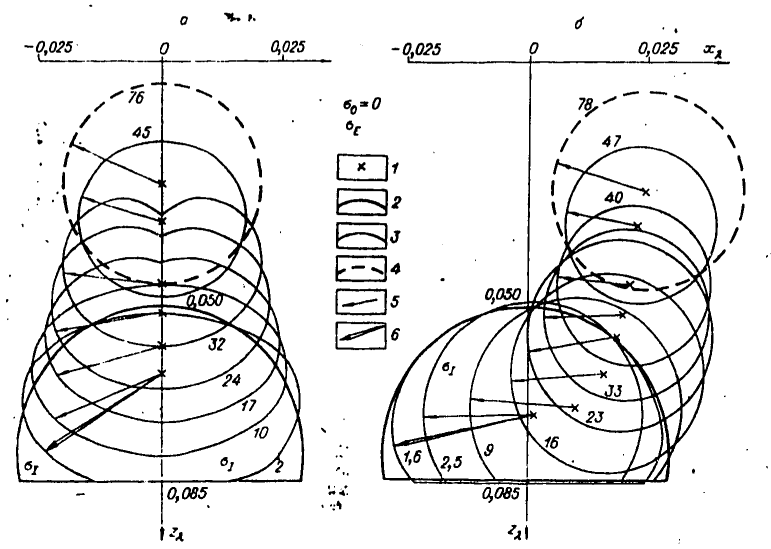

Fig. 3. Solution of the inverse problem by the "contracting surfaces method" with automatic correction of the position of the pole of the coordinate system. 1) current position of pole of coordinate system; 2) boundary of conducting inclusion; 3) initial approximations for each position of pole; 4) initial approximation; 5) indicator of initial approximation for each position of pole; 6) indicator of final result; the numbers on the curves represent the relative error of the approximation, %.

Figure 2 shows a model in which the homogeneous conducting earth contains a rectangular inclusion of anomalous conductivity. The inverse problem was solved by the "contracting surfaces method," first using the precise values of the space spectra of deep anomalous electromagnetic fields, and then using the values of the spectra, complicated by a 10% random error. The results presented in Fig. 2 show that despite the presence of a great error in the initial data, the interpretation in the second case, by means of the regularizing algorithm, makes it possible to solve the inverse problem almost with the same degree of accuracy as in the first case (with precise stipulation of the space spectra).

In the examples considered above, in accordance with the general theory of the method, the pole of the polar coordinate system (ρ, φ) was stipulated within the inhomogeneity $\hat{Q}$. If it is erroneous to stipulate it outside the inhomogeneity,

the iteration process leads to a solution which is sharply asymmetric relative to the pole and which does not reflect the true configuration of the $\hat{Q}$ region. However, in such a situation it is possible to make a correction to the position of the pole on the basis of an analysis of asymmetry of the contracting surfaces $\{f_i\}$. This operation is algorithmically realized in the following way. As an evaluation of the asymmetry of the function $f_i(\varphi)$ we use the expression

$$A[f_i] = \max_{\varphi \in [-\pi, \pi]} \frac{f_i(\varphi)}{f_i(\varphi - \pi)}. \tag{24}$$

In a case when

$$A[f_i] \geqslant \delta_1, \ \delta_1 = \text{const} > 1,$$

the pole is shifted from a point with the rectangular coordinates (ξ_0, ζ_0) to a point with the coordinates:

$$\xi_1 = \xi_0 + [f_i(\varphi_0) - f_i(\varphi_0 - \pi)] \cos \varphi_0,$$
$$\zeta_1 = \zeta_0 + [f_i(\varphi_0) - f_i(\varphi_0 - \pi)] \sin \varphi_0,$$

where φ_0 is the extremal value of the angle φ for expression (24) and the function f_i is scaled to a new pole (ξ_1, ζ_1). In a case when $A[f_i] < \delta_1$, the position of the pole does not change.

The effectiveness of the described procedure for correcting the position of the pole can be seen from the example shown in Fig. 3,a, where the initial information used was the values of the flux function for the magnetic field at the earth's surface caused by a semicylindrical inhomogeneity of conductivity σ_I, complicating a homogeneous half-space of conductivity σ_E. The initial approximation here was taken outside the anomalous body, but after a number of iterations we obtained an entirely satisfactory result. Figure 3,b shows the solution of a similar problem using a modified correction procedure in which for each new position of the pole the initial approximation is stipulated in the form of a circular cylinder equivalent in area to the area of the body obtained in the preceding iteration interval.

The cited examples show that the "contracting surfaces method" is quite resistant to errors in stipulation of the initial approximation and can be used both for determining the position of the geoelectric inhomogeneity and for more precise determination of its configuration.

BIBLIOGRAPHY

1. Berdichevskiy, M. N., Zhdanov, M. S., "Separation of the Variable Geomagnetic Field into Normal and Anomalous Parts," GEOMAGNETIZM I AERONOMIYA (Geomagnetism and Aeronomy), Vol 13, No 2, 1973.

2. Berdichevskiy, M. N., Zhdanov, M. S., Zhdanov, O. N., "Possibility of Separating Anomalies of the Variable Geomagnetic Field Into Surface and Deep Parts," GEOMAGNETIZM I AERONOMIYA, Vol 14, No 1, 1974.

3. Varentsov, I. M., "Approximate Method for the Mathematic Modeling of Electromagnetic Fields in Layered Media With Local Geoelectric Inhomogeneities," V VSESOYUZNAYA SHKOLA-SEMINARA PO ELEKTROMAGNITNYM ZONDIROVANIYAM (Fifth All-Union Seminar-School on Electromagnetic Soundings), Kiev, Naukova Dumka, 1978.

4. Glasko, V. B., Starostenko, V. I., "Regularizing Algorithm for Solution of a System of Nonlinear Equations in Inverse Problems in Geophysics," IZV. AN SSSR, FIZIKA ZEMLI (News of the USSR Academy of Sciences: Physics of the Earth), No 3, 1976.

5. Gol'mshtok, A. Ya., Zaytsev, V. B., Sochel'nikov, V. V., "Quantitative Evaluation of Convergence of the Successive Approximations Method for Solving an Integral Equation for E-Polarization," PRIKL. GEOFIZ. (Applied Geophysics), No 74, Moscow, 1974.

6. Dmitriyev, V. I., ELEKTROMAGNITNYYE POLYA V NEODNORODNYKH SREDAKH (Electromagnetic Fields in Inhomogeneous Media), MGU, 1969.

7. Dmitriyev, V. I., Barashnikova, I. A., Zakharov, Ye. V., ANOMAL'NYYE ELEKTROMAGNITNYYE POLYA PLASTOVYKH TEL (Anomalous Electromagnetic Fields of Stratified Bodies), Leningrad, Nedra, 1977.

8. Zhdanov, M. S., "Separation of the Earth's Variable Electromagnetic Fields," IZV. AN SSSR, FIZIKA ZEMLI (News of the USSR Academy of Sciences: Physics of the Earth), No 8, 1973.

9. Zhdanov, M. S., "Problems in the Theory of Interpretation of Deep Geomagnetic Anomalies," IZV. AN SSSR, FIZIKA ZEMLI, No 9, 1975.

10. Zhdanov, M. S., "Separation of Deep Electromagnetic Anomalies and Interpretation of Surface Anomalies," PRIKL. GEOFIZ., No 78, 1975.

11. Zhdanov, M. S., Berdichevskiy, M. N., Zhdanov, O. N., "Surface Anomalies of the Earth's Variable Electromagnetic Field," GEOMAGNETIZM I AERONOMIYA, Vol 15, No 3, 1975.

12. Kaufman, A. A., OSNOVY TEORII INDUKTIVNOY RUDNOY ELEKTRORAZVEDKI (Principles of the Theory of Inductive Ore Electrical Prospecting), Novosibirsk, Nauka, 1974.

13. Novikov, P.S., "Uniqueness of Solution of the Inverse Problem in Potential Theory," DAN SSSR (Reports of the USSR Academy of Sciences), Vol 18, No 3, 1938.

14. Ortega, Dzh., Reynboldt, V., ITERATSIONNYYE METODY RESHENIYA NELINEYNYKH SISTEM URAVNENIY SO MNOGIMI NEIZVESTNYMI (Iteration Methods for Solution of Nonlinear Systems of Equations With Many Unknowns), Moscow, Mir, 1975.

15. Rakitaki, T., ELEKTROMAGNETIZM I VNUTRENNEYE STROYENIYE ZEMLI (Electromagnetism and the Earth's Internal Structure), Leningrad, Nedra, 1968.

16. Rokityanskiy, I. I., Shuman, V. N., "Inverse Problem in Magnetovariation Profiling," IZV. AN SSSR, FIZIKA ZEMLI, No 8, 1971.

17. Tikhonov, A. N., Arsenin, V. Ya., METODY RESHENIYA NEKORREKTNYKH ZADACH (Methods for Solving Incorrect Problems), Moscow, Nauka, 1974.

18. Berdichevskiy, M. N., Dmitriev, V. I., "Distortion of Magnetic and Electrical Fields by Near-Surface Lateral Inhomogeneities," ACTA GEODAET., GEOPHYS. ET MOUNTANIST. ACAD. SCI. HUNG., 11(3-4), 1976.

19. Jones, F. W., Pascoe, L., "A General Computer Program for Determining the Perturbation of Alternating Electric Currents in a Two-Dimensional Model of Region of Uniform Conductivity With an Embedded Inhomogeneity," GEOPHYS. J. R. ASTR. SOC., 24, No 1, 1971.

20. Schmuker, U., "Interpretation of Induction Anomalies Above Nonuniform Surface Layers," GEOPHYSICS, 34, No 1, 1971.

21. Weidelt, P., "Inversion of Two-Dimensional Conductivity Structures," PHYS. EARTH AND PLANET INTERIORS, 10, No 3, 1975.

22. Weidelt, P., "Inversion of Two-Dimensional Conductivity Structures in E-Polarization: Proof of Uniqueness and Description of a Working Inverse Algorithm," IV WORKSHOP ON ELECTROMAGNETIC INDUCTION IN THE EARTH AND MOON, Murnau, FRG, 1978.

23. Zhdanov, M. S., CAUCHY INTEGRAL ANALOGUES FOR THE SEPARATION AND CONTINUATION OF ELECTROMAGNETIC INDUCTION IN THE EARTH AND MOON, Murnau, FRG, 1978.

5303
CSO: 1865/66

PHYSICS OF ATMOSPHERE

LOW-FREQUENCY WAVES AND SIGNALS IN THE EARTH'S MAGNETOSPHERE

Moscow NIZKOCHASTOTNYYE VOLNY I SIGNALY V MAGNITOSFERE ZEMLI in Russian 1980 (signed to press 10 Jul 80) pp 3-4, 153-156

[Foreword, table of contents and abstracts from collection "Low-Frequency Waves and Signals in the Earth's Magnetosphere", Izdatel'stvo "Nauka", 850 copies, 156 pages]

[Text] Foreword. This collection contains articles which discuss different aspects of investigations of low-frequency wave phenomena in magnetospheric plasma.

This problem is attracting interest due to the great quantity of important information concerning the parameters and state of the medium which were obtained in an analysis of low-frequency waves generated and propagating in near-earth plasma.

The complexity and uncertainty of the conditions under which the excitation and propagation of waves in near-earth plasma transpire make it difficult to understand and theoretically describe wave processes and their interrelationship to other phenomena. In particular, although the main generation mechanisms have been clarified, the onset and specific development of kinetic instability of plasma in particular situations and their consequences are still not thoroughly understood. This accounts for the great importance of experimental investigations which of necessity are becoming increasingly complex.

The surface registry of low-frequency radiations and signals alone affords no possibility for obtaining a full picture of these phenomena. The ionosphere plays the role of a singular filter through which some types of waves do not penetrate at all, and those which pass are highly distorted. In addition, in the case of surface observations a number of phenomena accompanying the excitation of radiations, in particular, changes in the state of energetic particles, can be traced only indirectly, on the basis of secondary effects (appearance of auroras, etc.). Satellite investigations are free of these restrictions. These have revealed important properties of the propagation and excitation of waves in near-earth plasma (unchannelized propagation, ionocyclotron wave branches, excitation at the frequency of the lower hybrid resonance, etc.) and for the first time information has been obtained on the absolute intensity of the radiations.

Despite the long-term history of investigations of low-frequency radiations and signals and the extensive literature on this problem many aspects of these phenomena still remain unclarified.

This collection contains articles which reflect the results of investigation of low-frequency electromagnetic radiations and signals registered primarily by artificial earth satellites. Under the "Intercosmos" program satellite wave experiments have been carried out at the Institute of Terrestrial Magnetism, Ionosphere and Radio Wave Propagation since 1970. In a series of such experiments it was possible to collect extensive material which is represented in a group of articles. The principal purpose of these studies is to make possible a full description of the amplitude and spectral characteristics of low-frequency radiations in the earth's outer ionosphere (200-1700 km) under different geomagnetic disturbance conditions. The information present in the world literature on this subject is fragmentary. Experiments on artificial earth satellites of the "Intercosmos" series made it possible to trace variations of radiations in connection with profound changes in the concentration of plasma in the main ionospheric gap and have led to a better understanding of changes in the intensity of radiations in this region of space.

The results of investigation of ionocyclotron whistlers, also registered on artificial earth satellites, are represented in their experimental-diagnostic and theoretical aspects in three articles.

The investigation of problems involved in the propagation of low-frequency waves is an indispensable aspect of study of wave processes in the magnetosphere. The propagation of low-frequency waves in inhomogeneous anisotropic magnetospheric plasma is also examined in the collection. Here important results were obtained by formulating a general algorithm for the computation of ray trajectories and changes in the amplitude of waves caused by their interaction with fluxes of high-energy electrons. This important step makes possible a more complete evaluation of the effects of unchannelized wave propagation not only on the basis of their penetration into different regions of the magnetosphere, but also on the basis of the energy effectiveness of such penetration.

During recent years active wave experiments have gained popularity. In these ionospheric and magnetospheric plasma are acted upon by low-frequency waves of a great intensity. Such dosed effects radically change the methods employed in wave experiments since to a considerable degree there is exclusion of the uncertainty in initial conditions and the possibility is afforded for artificially inducing a whole series of phenomena (excitation of micropulsations, particle diffusion, etc.). Some results of study of nonlinear phenomena carried out at the Institute of Terrestrial Magnetism, Ionosphere and Radio Wave Propagation in collaboration with a number of other institutes are also presented in the collection.

For a better understanding of the conditions for carrying out wave experiments on artificial earth satellites a table gives information on the satellites used and the observation program employed (see Appendix).

The authors of the collection feel it mandatory to note that they have cooperated with many specialists from different institutes in the Soviet Union and abroad. The friendly support from them and useful discussions were very productive. The authors express appreciation to all the persons on whose assistance they depended.

Ya. I. Likhter

CONTENTS

ABSTRACTS

UDC 551.510.535

SPATIAL-TEMPORAL VARIATIONS OF ELF AND VLF RADIATIONS IN THE EARTH'S OUTER IONOSPHERE

[Abstract of article by Likhter, Ya. I., and Larkina, V. I.]

[Text] This is a discussion of the results of analysis of spatial-temporal variations of the properties of ELF and VLF radiations in the outer ionosphere on the basis of experimental data obtained using some artificial earth satellites of the "Intercosmos" series. There was found to be a difference in the diurnal variations of ELF and VLF radiations under quiet conditions and their similarity under disturbed conditions. It was established that there is a dependence between the amplitude of LF radiations on the L-shell under different conditions of geomagnetic disturbance. The already enumerated regularities and also the asymmetry of the ELF radiations in the northern and southern hemispheres confirm the hypothesis of excitation of part of the ELF radiations at ionospheric altitudes. Figures 16, tables 1, references 33.

UDC 551.510.535

NOISE RADIATIONS IN THE OUTER IONOSPHERE AND GEOMAGNETIC STORMS

[Abstract of article by Likhter, Ya. I., and Larkina, V. I.]

[Text] This article is devoted to an analysis of the behavior of noise LF radiations in the outer ionosphere at the time of geomagnetic storms. Variations in the amplitude of ELF and VLF radiations in the course of development of a number of storms are traced in detail. It was discovered that variations in the amplitude of radiation during each magnetic storm have their distinguishing characteristics and differ in some respects from other storms. Depending on storm intensity there is a change in: the amplitude of the radiation, minimum L-shell to which the maximum of the amplitude of the radiation descends in the main phase of the storm and the time during which the radiation maximum after a storm again returns to L = 4-5. The apparent variations of ELF and VLF radiations during individual storms and substorms can differ substantially. These characteristics can be attributed to both storm intensity and the level of disturbance at which the storm (substorm) began. Figures 12, tables 3, references 16.

UDC 551.510.535

INVESTIGATION OF THE INTENSITY SPECTRA OF ELF AND VLF RADIATIONS

[Abstract of article by Zakharov, A. V., Likhter, Ya. I., and Kuznetsov, S. N.]

[Text] This is a discussion of the averaged spectra of ELF and VLF radiations measured on the "Intercosmos-5" artificial earth satellite in the earth's outer ionosphere with $L \leqslant 4.7$. The frequencies of the spectral maxima vary in dependence on L proportional to: a) the gyrofrequency of electrons at the equator, b) the lower hybrid frequency at the equator and c) the gyrofrequency of protons at satellite flight altitude. The intensity of ELF and VLF radiations measured in the outer ionosphere are compared with the intensity measured on high-apogee satellites. Figures 5, references 18.

UDC 551.510.535

VARIATIONS IN THE INTENSITY AND SPECTRUM OF ELF AND VLF RADIATIONS IN THE MAIN IONOSPHERIC GAP

[Abstract of article by Gdalevich, G. L., Likhter, Ya. I., Larkina, V. I., and Mikhaylov, Yu. M.]

[Text] The article gives an analysis of variations of the spectrum and amplitude of ELF and VLF radiations in the zone of the main ionospheric gap, together with changes in the structural parameters of the gap. With entry into the gap, with a decrease in the concentration of plasma and an increase in the electron temperature, there is a decrease in the lower boundary frequency of the noise band. At altitudes greater than 1,000 km the amplitude of the electric and magnetic field components increases considerably in the region where the plasma concentration is minimum. An analysis of the ratio of the amplitudes of the magnetic and electric components of the field of ELF radiations is evidence of the electromagnetic nature of the corresponding waves. It can also be assumed that in these regions there is a considerable admixture of electrostatic waves, evidently of a local origin. Figures 6, tables 1, references 34.

UDC 551.510.535

ANALYSIS OF THE INFLUENCE OF GEOPHYSICAL CONDITIONS ON THE APPEARANCE OF VLF CHORUSES IN MAGNETICALLY CONJUGATE SUBAURORAL REGIONS

[Abstract of article by Smirnova, N. A., Novikov, Yu. P., Natsvalyan, L. A.]

[Text] The following regularities were revealed from an analysis of VLF choruses at subauroral magnetically conjugate observatories, Sogra and Kerguelen ($L \sim 3.7$). With an increase in magnetic activity and under conditions of a disturbed ionosphere there is an increase in the probability of appearance of conjugate (registered at both observatories) VLF choruses. The maximum of the frequency of appearance of nonconjugate (registered at one of the observatories) choruses is displaced to later hours relative to the maximum of the appearance of conjugate choruses. The probability of appearance of nonconjugate choruses is greater at that observatory where the dawn occurs earlier (Kerguelen Observatory). The probability of appearance of conjugate choruses increases when the observatory is projected into a region outside the plasmosphere. It is shown that the noted regularities can be satisfactorily explained within the framework of creation of optimum conditions for the generation of VLF choruses due to the development of cyclotron instability with the filling of the equatorial regions of the magnetosphere with cold plasma and favorable conditions for the penetration of radiation to the earth's surface, associated with the presence of ionization inhomogeneities in the ionosphere. Figures 5, references 6.

UDC 550.388.2

DIAGNOSIS OF THE OUTER IONOSPHERE USING IONOCYCLOTRON WHISTLERS

[Abstract of article by Sobolev, Ya. P.]

[Text] An analysis of ionocyclotron whistlers registere on artificial earth satellites makes it possible to determine the relative composition of different species of ions at altitudes from 500 km and above. The author gives the corresponding results on the basis of data from the artificial earth satellite "Intercosmos-5." The diagnostic possibilities of ionocyclotron noise received aboard the artificial earth satellite "Intercosmos-14" are given. Figures 12, tables 1, references 20.

UDC 550.388

AMPLITUDE SPECTRUM OF IONOCYCLOTRON WHISTLERS NEAR THE IONIC GYROFREQUENCY IN THE UPPER IONOSPHERE

[Abstract of article by Bud'ko, N. I.]

[Text] A study was made of the behavior of the amplitude spectrum of the magnetic field of ionocyclotron whistlers near the ionic gyrofrequency under the conditions prevailing in the upper ionosphere. An increase in the refractive index with approach to the gyrofrequency leads to a slow increase in amplitude, near the gyrofrequency cyclotron absorption rapidly cuts off this increase, and a characteristic maximum appears in the neighborhood of the ionic gyrofrequency in the amplitude spectrum. A knowledge of the position of the maximum in the spectrum can be used in determining the temperature of the "tail" of the distribution of ions or estimating the nonequilibrium nature of the distribution function. Figures 1, references 10.

UDC 550.388

STANDARD SOLUTION OF THE PROBLEM OF TRANSFORMATION OF AN ORDINARY WAVE INTO AN EXTRAORDINARY WAVE IN A LOW-FREQUENCY CASE

[Abstract of article by Ryabov, B. S.]

[Text] In the approximation of a weak correlation between incident and reflected waves the author has obtained a standard solution of the problem of the transformation of an ordinary wave into an extraordinary wave in nonabsorbing plasma containing not less than two species of ions in a low-frequency case. This solution makes it possible to compute not only the amplitudes and phases of the transformation coefficients, but also the value of the field of waves in the field of interaction itself. In the case of practical importance of strong interaction of waves the author has found the characteristic spatial and frequency scales of transformation and gives their numerical estimates for the outer ionosphere. It is postulated that the branching frequencies determined experimentally from the spectra of the observed signals of electron and ionocyclotron whistlers are understated. References 9.

UDC 550.388.2

QUASISTATIC, ELF AND VLF ELECTRIC FIELDS IN THE REGION OF THE MAIN IONOSPHERIC GAP

[Abstract of article by Mikhaylov, Yu. M., Klimov, S. I., and Savin, S. P.]

[Text] A study was made of a complex of electric measurements in the range 0.03-$20 \cdot 10^3$ Hz when using the artificial earth satellite "Intercosmos-10." The authors investigated the spatial-temporal relationships between the noise of the lower hybrid resonance and quasistatic electric fields (0.03-70 Hz) in the region of the main ionospheric gap. Under conditions of stability of the structure of the gap the spatial-temporal distribution of noise of the lower hybrid resonance also remained stable. The article discusses the possibility of the excitation of electromagnetic oscillations in the range of the lower hybrid resonance by transverse fluxes of ions caused by quasistatic electric fields in plasma. Figures 3, tables 1, references 13.

UDC 550.388

MODULATION OF ELECTRIC CURRENTS IN THE IONOSPHERE BY A POWERFUL VLF WAVE

[Abstract of article by Molchanov, O. A., and Shchekotov, A. Yu.]

[Text] The article examines the mechanism of the appearance of radiation at the frequency of modulation of a powerful VLF wave propagating through high-latitude ionospheric plasma with an electrojet. Allowance for the nonuniformity of the field of the heating wave leads to the appearance of optimum frequencies in the range 3-30 Hz. Theoretical estimates are supported by experimental results. References 12.

UDC 550.388

MODELING OF THE PROCESS OF AMPLITUDE CHANGES OF VLF WAVES IN THE EARTH'S PLASMOSPHERE

[Abstract of article by Mal'tseva, O. A., Molchanov, O. A., and Reznikov, A. Ye.]

[Text] Algorithms for computing the amplitude of VLF waves in the earth's magnetosphere in a linear approximation with allowance for the effects of kinetic attenuation, defocusing and change in polarization are described. The results of the computations are compared with data from registry of signals of a VLF transmitter in a magnetically conjugate region and with the VLF radiations at $f \gtrsim f_{LHR}$ observed on artificial earth satellites. Figures 17, references 36.

UDC 621.396.674

DIRECTIONAL DIAGRAM OF RECEIVING DIPOLE ANTENNAS IN MAGNETICALLY ACTIVE PLASMA

[Abstract of article by Likhter, Ya. I.]

[Text] In most wave experiments on an artificial earth satellite use is made of one or two magnetic or electric dipole antennas. The article gives an analysis of the ratio of the amplitudes of the components measured in such experiments to the total amplitude of the field components (directional diagram). It is shown that the directional diagram of magnetic and electric receiving antennas in magnetically active plasma is determined by the frequency of the wave and by its direction of propagation, as well as the orientation of the antennas relative to the magnetic field (axis of anisotropy) and the wave normal. Usually the measured values are less than or considerably less than the total amplitude of the field components and are equal to them only in special cases. It is deemed desirable that measurements be made on satellites oriented in the magnetic field. Figures 5, references 22.

UDC 550.388

GROUP VELOCITY OF WHISTLERS IN HOT ANISOTROPIC PLASMA

[Abstract of article by Varshavskiy, S. P., Polyavin, D. I., and Sazhin, S. S.]

[Text] The authors examine the influence of anisotropy of the electron distribution function on the group velocity of whistlers propagating along the magnetic field. It is shown that in the case of a distribution function elongated in the direction of small pitch angles its anisotropy leads to an increase in the "temperature effect" on the group velocity. In the case of a distribution function elongated in the direction of large pitch angles the anisotropy leads to the compensation of the "temperature effect" in such a way that with some anisotropy and wave frequency the group velocity coincides with the expression derived from the model of cold plasma. It is shown that for frequencies close to 0.9 of the electron gyrofrequency the group velocity can change by an order of magnitude with changes in the anisotropy of the electron distribution function acceptable for real magnetospheric conditions. Figures 3, references 9.

UDC 550.388

REFLECTION OF WAVES NORMALLY INCIDENT ON AN INHOMOGENEOUS ANISOTROPIC IONOSPHERE IN THE NEIGHBORHOOD OF THE LOWER HYBRID FREQUENCY

[Abstract of article by Kaufman, R. N.]

[Text] In a quasilongitudinal approximation a study was made of the frequency dependence of the reflection coefficients for waves normally incident on an inhomogeneous ionosphere in the neighborhood of the lower hybrid frequency. It is shown that the modulus of the reflection coefficients in this neighborhood have extrema. Figures 2, references 6.

END

5303
CSO: 1865/97